

Sensitive Detection of Phosphorus Deficiency in Plants Using Chlorophyll *a* Fluorescence¹

Jens Frydenvang^{2*}, Marie van Maarschalkerweerd², Andreas Carstensen², Simon Mundus, Sidsel Birkelund Schmidt, Pai Rosager Pedas, Kristian Holst Laursen, Jan K. Schjoerring, and Søren Husted*

Department of Plant and Environmental Sciences, Faculty of Science, University of Copenhagen, 1871 Frederiksberg C, Denmark (J.F., M.v.M., A.C., S.M., S.B.S., P.R.P., K.H.L., J.K.S., S.H.); and FOSS Analytical A/S, 3400 Hillerød, Denmark (M.v.M.)

ORCIDIDs:0000-0001-9294-1227(J.F.);0000-0002-2748-3239(M.v.M.);0000-0001-5029-7015(A.C.);0000-0002-2128-8061(S.M.);0000-0002-4193-4454(S.B.S.);0000-0001-6733-7300(P.R.P.);0000-0001-7900-3324(K.H.L.);0000-0002-2852-3298(J.K.S.);0000-0003-2020-1902(S.H.).

Phosphorus (P) is a finite natural resource and an essential plant macronutrient with major impact on crop productivity and global food security. Here, we demonstrate that time-resolved chlorophyll *a* fluorescence is a unique tool to monitor bioactive P in plants and can be used to detect latent P deficiency. When plants suffer from P deficiency, the shape of the time-dependent fluorescence transients is altered distinctively, as the so-called I step gradually straightens and eventually disappears. This effect is shown to be fully reversible, as P resupply leads to a rapid restoration of the I step. The fading I step suggests that the electron transport at photosystem I (PSI) is affected in P-deficient plants. This is corroborated by the observation that differences at the I step in chlorophyll *a* fluorescence transients from healthy and P-deficient plants can be completely eliminated through prior reduction of PSI by far-red illumination. Moreover, it is observed that the barley (*Hordeum vulgare*) mutant *Viridis-zb*⁶³, which is devoid of PSI activity, similarly does not display the I step. Among the essential plant nutrients, the effect of P deficiency is shown to be specific and sufficiently sensitive to enable rapid in situ determination of latent P deficiency across different plant species, thereby providing a unique tool for timely remediation of P deficiency in agriculture.

The world population is estimated to exceed 9 billion people by 2050. This means that agriculture on a global scale has to increase food production by 70% to 100%, and, at the same time, handle the consequences of global climate changes and reduce its environmental footprint (Food and Agriculture Organization of the United Nations, 2009; Godfray et al., 2010; Foley et al., 2011). A major challenge related to this is the supply and use of phosphorus (P) to support future plant production (Cordell et al., 2009; Gilbert, 2009; MacDonald et al., 2011).

P is an essential plant nutrient, which means that plants require P in adequate amounts to fulfill a complete

lifecycle. It has been estimated that 30% of the world's agricultural soils are P deficient and need fertilizer addition to ensure yield and quality (MacDonald et al., 2011). However, phosphate rock, the main source of P fertilizers, is a finite natural resource, and the known rock phosphate reserves are estimated to last as little as 50 years in the gloomiest forecasts (Gilbert, 2009; Edixhoven et al., 2013). This makes P a potential strategic natural resource similar to oil, as very few countries control the vast majority of the known reserves (Gilbert, 2009; Elser and Bennett, 2011; Edixhoven et al., 2013). Presently, an immense overuse of P is found in some parts of the world, causing eutrophication of lakes and seas, while P depletion results in severe yield limitations elsewhere (MacDonald et al., 2011; Obersteiner et al., 2013). An essential aspect of solving both of these problems is to increase P use efficiency in agriculture, thus reducing the negative environmental impact of agriculture and helping to ensure a sustainable use of P resources while increasing the worldwide food production (Schröder et al., 2011; Veneklaas et al., 2012).

Here, we present a unique analytical principle based on chlorophyll *a* fluorescence that allows rapid, non-destructive, onsite assessment of plant P status by recording the so-called OJIP transient of a dark-adapted leaf.

When a chlorophyll molecule absorbs light, one of three events will occur: The light may be used to drive photosynthesis, it can be dissipated as heat, or it can be

¹ This work was supported by the Danish Strategic Research Council (NUTRIEFFICIENT; grant no. 10-093498), Foss Analytical A/S, Innovation Fund Denmark, and the University of Copenhagen.

² These authors contributed equally to the article.

* Address correspondence to jfr@plen.ku.dk and shu@plen.ku.dk.

The author responsible for distribution of materials integral to the findings presented in this article in accordance with the policy described in the Instructions for Authors (www.plantphysiol.org) is: Søren Husted (shu@plen.ku.dk).

J.F., M.v.M., A.C., and S.H. designed the experiments and performed the fluorescence measurements and multivariate analysis; A.C. and S.M. performed and evaluated field trials; S.B.S., K.H.L., and P.R.P. performed and evaluated fluorescence measurements on plants exposed to nutrient deficiencies other than phosphorus; all authors participated in data interpretation and in writing the final article.

www.plantphysiol.org/cgi/doi/10.1104/pp.15.00823

reemitted as fluorescence. Less than 10% of light absorbed by the plant causes emission of chlorophyll *a* fluorescence (Govindjee, 2004; Stirbet and Govindjee, 2011). When a dark-adapted leaf is exposed to saturating actinic light, the resulting time-dependent fluorescence forms a so-called Kautsky curve (Kautsky and Hirsch, 1931; McAlister and Myers, 1940). Within 300 ms, the fluorescence increases from a minimum level (F_0) to the maximum level. If measured with a sufficiently high time resolution, a polyphasic transient with four distinct steps, designated as O, J, I, and P, is observed. After reaching maximum intensity at the P step, the fluorescence intensity declines until it reaches a steady state within a few minutes (Harbinson and Rosenqvist, 2003; Govindjee, 2004).

The physiological mechanisms underlying the polyphasic OJIP transient are still not clarified, but it is believed that the J and I steps represent dynamic bottlenecks in the photosynthetic electron transport chain. The first rise (2 ms) from O to J is referred to as the photochemical phase due to its dependence on the intensity of the incoming light. This phase is assumed to reflect the reduction of the primary quinone electron acceptor in PSII (Stirbet and Govindjee, 2011). The reduction of the primary quinone electron acceptor results in a decreased electron trapping efficiency and therefore an increase in the dissipation of absorbed light energy by fluorescence and heat. The second part, from J over I to P, is called the thermal phase due to its temperature sensitivity. This phase is much slower than the first, and it is believed that the J-I phase primarily reflects a sequential reduction of the remaining plastoquinone pool of PSII and that the I-P phase reflects the subsequent electron flow through cytochrome *b₆f* to electron sinks at the PSI acceptor side (Stirbet and Govindjee, 2011). Thus, the OJIP transient resembles a titration of the photochemical quantum yield and reflects the complex electron transport properties of PSII and PSI.

Consistent with their known influence on photosynthesis, deficiencies of essential plant nutrients such as Fe, Cu, Mg, Mn, and S have previously been shown to affect OJIP transients (Kastori et al., 2000; Mallick and Mohn, 2003; Larbi et al., 2004; Husted et al., 2009; Tang et al., 2012; Yang et al., 2012). As a consequence, several attempts have been made to identify nutrient imbalances and disorders using one or several parameters derived from the transients, but apart from Mn (Husted et al., 2009; Schmidt et al., 2013), attempts have not been successful in terms of sensitivity and specificity. This includes P, which previously has been reported to have an effect on OJIP transients, yet the reported effects seem mutually contradictory and nonspecific to P (Ripley et al., 2004; Weng et al., 2008; Jiang et al., 2009; Lin et al., 2009).

Here, we present the unique finding that increasing levels of P deficiency affect the shape of the OJIP transient around the I step at 20 to 50 ms and causes the I step to gradually straighten and disappear. It is demonstrated that this effect is fully reversible and, among

the essential plant nutrients, specific for P deficiency using both monocotyledons (barley [*Hordeum vulgare*]) and dicotyledons (tomato [*Solanum lycopersicum*]) plant species. Furthermore, it is shown that it is possible to determine whether a plant is P sufficient or deficient and to quantitatively predict the P concentration in leaf tissue using multivariate analysis of the OJIP transients.

RESULTS

Chlorophyll *a* Fluorescence Measurements Show Characteristic OJIP Transients in P-Deficient Plants

The ability of chlorophyll *a* fluorescence measurements to quantitatively predict the bioactive concentration of P in leaves was investigated in experiments with hydroponically and soil-grown barley and tomato plants. The different growth regimes resulted in plants spanning the full range of foliar P concentrations, from luxury P uptake ($>4,000 \mu\text{g P g}^{-1}$ dry weight [DW]) to severe P deficiency ($<1,000 \mu\text{g P g}^{-1}$ DW; Supplemental Table S1). No visual symptoms of P deficiency were observed on the leaves except for a marginal anthocyanin production on the most P-deficient plants. However, typical signs of latent P deficiency were found (Fig. 1), including increased root to shoot ratio, decreased tillering, reduced biomass, and only slightly decreased chlorophyll concentrations (Supplemental Table S2). Carotenoid concentrations were not significantly affected, and element analysis of the leaves showed that the plants suffered from no additional

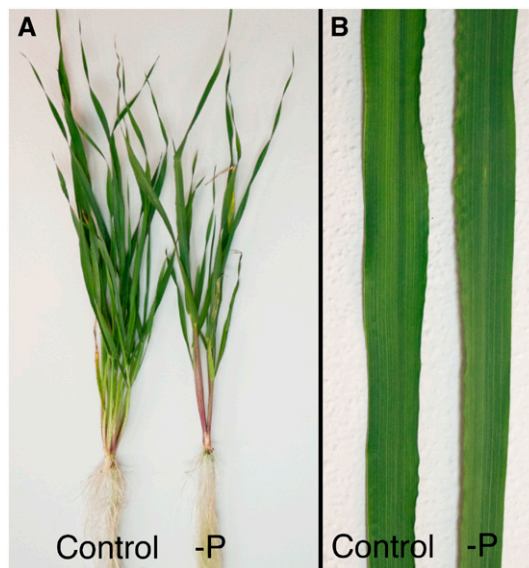


Figure 1. Control and P-deficient barley plants grown in hydroponics. A, Increased root to shoot ratio and a decrease in tillering and shoot weight are evident for the P-deficient plant compared with the healthy control plant. B, No symptoms were visible on the youngest fully developed leaves of control versus P-deficient plants, indicating latent P deficiency.

nutrient deficiencies other than P (Supplemental Table S1). The visual signs of P deficiency would therefore only be noticed if plants could be directly compared to control plants of similar age, thus making in situ visual diagnosis practically impossible.

OJIP transients measured on the youngest fully developed leaf (YFDL) of hydroponically grown control plants with sufficient P status showed normal poly-phasic transients with four distinct steps (Fig. 2). By contrast, P-deficient plants showed deviating OJIP curves in which the I step measured at 20 to 50 ms straightened and almost completely vanished, whereas the shapes of the O, J, and P steps appeared unaffected (Fig. 2).

The appearance of the I step depended dynamically on the P status of the barley plants. Thus, the I step was observable in 21-d-old plants (Fig. 3) that had attained a moderate P deficiency ($1,200 \mu\text{g P g}^{-1} \text{ DW}$ in YFDL; Supplemental Table S1; Reuter et al., 1997). However, as the plants gradually became more severely P deficient, the I step completely disappeared (28-d-old plants with $900 \mu\text{g P g}^{-1} \text{ DW}$ in YFDL; Fig. 3). Resupply of P to the nutrient solution to the 28-d-old plants caused the I step to reappear to control levels within 2 d (30-d-old plants; Fig. 3). A faster recovery was observed when incubating a P-deficient leaf in a P solution. Here, the I step started to reemerge within 30 min, and a full reappearance was seen within 120 min (Supplemental Fig. S1).

Consistent with P being a phloem-mobile nutrient (Hawkesford et al., 2012), the effect of P deficiency was observed in the second YFDL prior to being observed in the YFDL (Supplemental Fig. S2A).

Joly et al. (2010) reported that applying a far-red light pulse to specifically reduce PSI prior to measuring the OJIP transient of dark-adapted leaves resulted in a

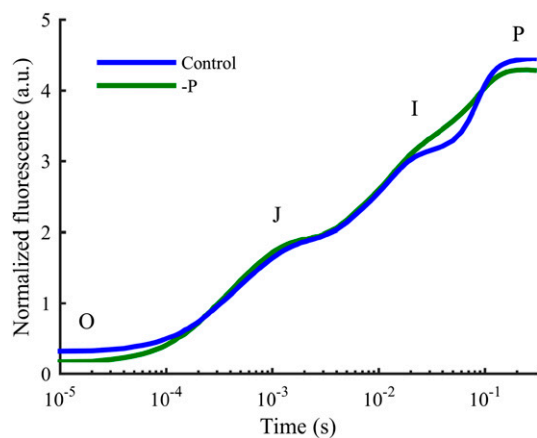


Figure 2. Typical OJIP transients from a healthy control (blue) and a P-deficient (green) barley plant. The I step is seen to have straightened and disappeared in the OJIP transient from the P-deficient plant, whereas the shape of the O, J, and P are unaffected. The OJIP transients, measured in arbitrary units (a.u.), have been normalized by F_0 and subjected to the curve correction as described in “Materials and Methods.”

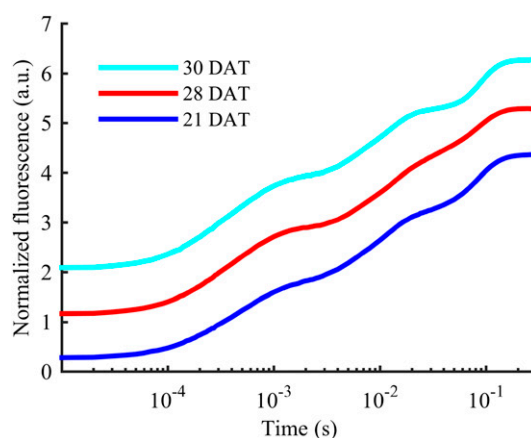


Figure 3. OJIP transients for the YFDL of a barley plant growing at the lowest level of P supply. Each transient has been offset by 1 arbitrary unit (a.u.) to improve legibility. It is seen that the I step gradually straightens and disappears as plants become increasingly P deficient from 21 DAT ($1,200 \mu\text{g P g}^{-1} \text{ DW}$) to 28 DAT ($900 \mu\text{g P g}^{-1} \text{ DW}$). Two days after plants were resupplied with P at 28 DAT, the I step had reappeared to a control-like state.

fading of the I step. Subjecting both P-deficient and healthy control barley leaves to a 60-s far-red light pulse prior to measuring the OJIP transients (Supplemental Fig. S2B) led to a complete elimination of the observed difference between healthy and P-deficient plants when measured without prior reduction of PSI (Fig. 2).

Similarly, the barley mutant *Viridis-zb⁶³* has been shown to be almost completely devoid of PSI activity (Nielsen et al., 1996). While the OJIP transients show very low maximum fluorescence, the preprocessing allows for comparing the shape of the OJIP transients measured from the *Viridis-zb⁶³* mutant to OJIP transients from a control plant. Doing so, it is clearly observed that the I step is completely absent in the OJIP transient from the *Viridis-zb⁶³* mutant (Supplemental Fig. S2C).

Predicting the Bioactive P Concentration in Barley Leaves

The chlorophyll *a* fluorescence measurements on the YFDL of barley plants grown in both hydroponics and in soil resulted in a data set with 701 OJIP transients. All OJIP transients were normalized by F_0 and subjected to a correction, allowing differences in the overall slope and offset of the transients to be normalized across all experiments. Thereafter, the transients were differentiated, scaled and, smoothed to augment the observed straightening of the I step (Supplemental Fig. S3). The resulting preprocessed OJIP transients were used for development and testing of a partial least-squares regression (PLS) model predicting the P concentration in each leaf.

The development and calibration of the PLS model was based on the first 300 ms (i.e. up to the P step) of OJIP transients measured on hydroponically grown

barley plants in experiment 1 (see “Materials and Methods”). During the development of the model, it became evident that the OJIP transients appeared not to respond to high P concentrations. Including leaves with concentrations up to $3,600 \mu\text{g P g}^{-1} \text{ DW}$, a total of 159 OJIP transients provided the basis for development of a PLS model with a low prediction error (Fig. 4A) that successfully predicted concentrations up to the sufficiency range for barley at $3,000 \mu\text{g P g}^{-1} \text{ DW}$ (Reuter et al., 1997).

For validation of the PLS model, 291 OJIP transients measured in three completely independent experiments including soil- and hydroponically cultivated barley plants (experiments 2, 3, and 4) were taken into

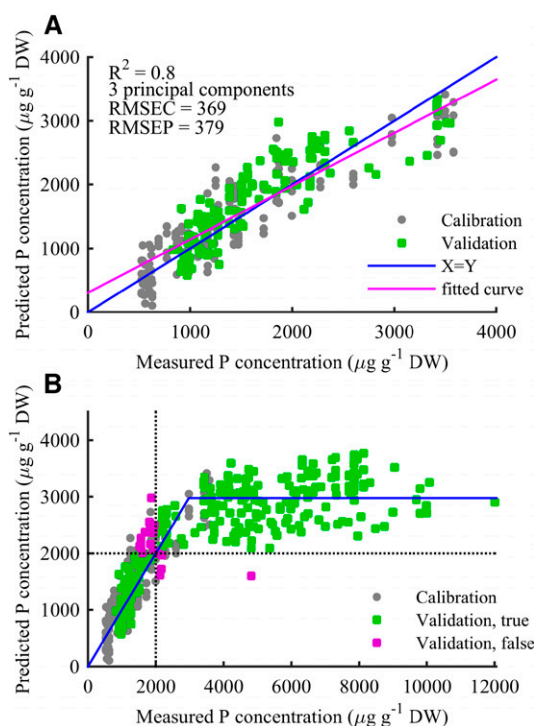


Figure 4. Predicted versus measured barley leaf P concentrations based on a PLS model with three principal components. A, PLS prediction in the calibration range. Gray circles indicate calibration samples, and red circles indicate validation samples. The blue curve indicates the optimal $Y = X$ line, and the red curve represents best linear fit to data ($R^2 = 0.8$). The root-mean-squared error for the 159 calibration samples (root-mean-squared error of calibration [RMSEC] = 369) is seen to be very equivalent to the root-mean-squared error for the 131 independent test samples (root-mean-squared error of prediction [RMSEP] = 379). Together with the low number of principal components used, this shows that the model is not a result of overfitting. B, Predicted versus measured P concentrations for all 448 OJIP transients. The blue curve represents the optimal fit of a $Y = X$ line intersecting a constant line at $2,975 \mu\text{g g}^{-1} \text{ DW}$. The two dotted lines indicate $2,000 \mu\text{g g}^{-1} \text{ DW}$, and coloring indicates whether the PLS model predicts samples correctly according to this threshold. Two hundred sixty-nine of 291 leaves (92%) from the test set were correctly classified as above or below the $2,000 \mu\text{g g}^{-1} \text{ DW}$ threshold, and the misclassified leaves position close to the threshold except for one measurement.

account. Of these transients, 131 fell within the 0 to $3,600 \mu\text{g P g}^{-1} \text{ DW}$ concentration range. To minimize overfitting, a very rigorous cross-validation procedure was used in which one-half of the calibration transients were excluded in each cross-validation step. Three principal components were found to be optimal for predicting the leaf P concentrations (Fig. 4A). This limited number of principal components taken together with very comparable root-mean-squared error of calibration (369) and root mean squared error of prediction (379) for the validation transients (Fig. 4A) revealed that overfitting was not a problem. Furthermore, the regression vector for the PLS model (Supplemental Fig. S4) showed that the predictions were dependent on the straightening of the I step, thus providing evidence that the PLS model reflected the initial observations of the straightening of the I step when plants become P deficient.

The developed model was thereafter used to predict leaf P concentrations for the calibration data set as well as for all 289 OJIP transients in the validation data set with P concentration up to more than $10,000 \mu\text{g P g}^{-1} \text{ DW}$. Plotting the predicted versus the measured P concentrations clearly showed that the model was able to accurately predict leaf P concentrations at deficient levels, while leaves with a higher P concentration were predicted to an apparently constant value (Fig. 4B). Using a least-squares method to fit the intersect between a line representing an accurate PLS prediction ($Y = X$) and a constant prediction ($Y = \text{constant}$) gave a cutoff value of $2,975 \mu\text{g g}^{-1} \text{ DW}$ (blue curve in Fig. 4B).

Field trials suggest that a leaf P concentration below $2,000 \mu\text{g g}^{-1} \text{ DW}$ in the YFDL of 30-d-old barley plants leads to grain yield loss (Supplemental Table S3). For comparison, no yield losses were observed when the leaf P concentration of the YFDL was $2,300 \mu\text{g g}^{-1} \text{ DW}$ or higher. Setting a threshold at $2,000 \mu\text{g g}^{-1} \text{ DW}$, the generated PLS model was able to correctly classify 269 out of the 291 leaves (92%) in the validation set as either P deficient or sufficient (Fig. 4B). For the 22 misclassified leaves, the actual measured P concentration was very close to the $2,000 \mu\text{g P g}^{-1} \text{ DW}$ threshold, except for one leaf measured to have a concentration above $4,000 \mu\text{g g}^{-1} \text{ DW}$ but predicted below $2,000 \mu\text{g g}^{-1} \text{ DW}$. This leaf was from a soil-grown plant resupplied with P.

Specificity of the P Effect

To test whether the observed effect of P deficiency was specific to P among other essential plant nutrients, a principal component analysis (PCA) model was developed for OJIP transients collected in this experiment as well as in previous experiments (Hebborn et al., 2009; Husted et al., 2009; Schmidt et al., 2013). In these studies, OJIP transients were measured on barley and tomato plants exposed to Ca, Cu, Fe, K, Mg, Mn, N, P, S, or Zn deficiency, along with healthy control plants.

Consistent with the previously reported strong effect of Mn on chlorophyll *a* fluorescence transients (Husted et al., 2009), Mn-deficient leaves dominated the variance described by the PCA and were clearly distinguishable from other deficiencies in the first principal component explaining 73% of the variance (Supplemental Fig. S5). However, observing principal components 2 and 5 (Fig. 5), it was evident that the P-deficient leaves from all experiments (including both barley and tomato leaves) clustered in the first quadrant of this subspace and that this group could be separated from all other nutrient deficiencies. Furthermore, S-deficient leaves clustered in the third quadrant of the same principal component subspace, and Cu-deficient leaves clustered on the border between the first and fourth quadrant. Considering the strong effect of Mn deficiency on OJIP transients, it was not surprising that the explained variance of the principal component subspace showing a P clustering only constituted 12.6% of the total variation (Fig. 5).

Looking at the loadings for principal components 2 and 5 (Supplemental Fig. S6), it was evident that principal component's 2 and 5 depended greatly on the I step of the OJIP transient, further corroborating the connection between a fading I step and P deficiency. Comparing the OJIP transients from P-deficient plants to those from S- and Cu-deficient plants (Supplemental Fig. S7), it was clear that while the I step was affected, the change of shape was distinctly different compared with the P-deficient plants. From the unprocessed fluorescence transients (Supplemental Fig. S7), S deficiency seemed to cause a more pronounced I step compared with even the control curves. For Cu-deficient plants, it appeared that the P step in particular was lowered, leading to a cutoff rather than a step at the I step.

DISCUSSION

P Deficiency and the Fading I Step

A straightening and gradual fading of the I step of the polyphasic OJIP transients was observed when plants were exposed to increasing severity of P deficiency (Fig. 3). P has several key functions in plants, including a structural role in nucleic acids, biomembranes, and NADPH and ATP syntheses as well as in regulation of metabolism via phosphorylation (Hawkesford et al., 2012). Despite these essential roles, P deficiency has not previously been shown to have a direct impact on the photosynthetic electron transport chain (Engels et al., 2012; Hawkesford et al., 2012) and hence on the OJIP transients, apart from experiments with severely P-deficient plants, which causes chlorophyll loss and decreased maximum quantum yield of PSII due to photooxidative stress (Hernández and Munné-Bosch, 2015).

Changes in the I-P phase of OJIP transients indicate an effect on the photosynthetic electron transport chain beyond cytochrome *b₆f* (Pospíšil and Dau, 2002; Schansker et al., 2005; Joly and Carpentier, 2007; Antal and Rubin, 2008; Laisk et al., 2009). Furthermore, the observed elimination of the differences between OJIP transients from control and P-deficient plants with prior reduction of PSI using far-red light (Supplemental Fig. S2B; Joly et al., 2010) indicates a linkage between P deficiency and the electron transport in the vicinity of PSI (Schansker et al., 2005). This linkage is also supported by the observation that the I step is completely absent in OJIP transients from *Viridis-zb⁶³* mutant (Supplemental Fig. S2C). The sigmoidal rise of the I-P phase may accordingly result from a dynamic bottleneck involving a transient inactivation of ferredoxin-NADP⁺ reductase by carbon metabolites of the Calvin

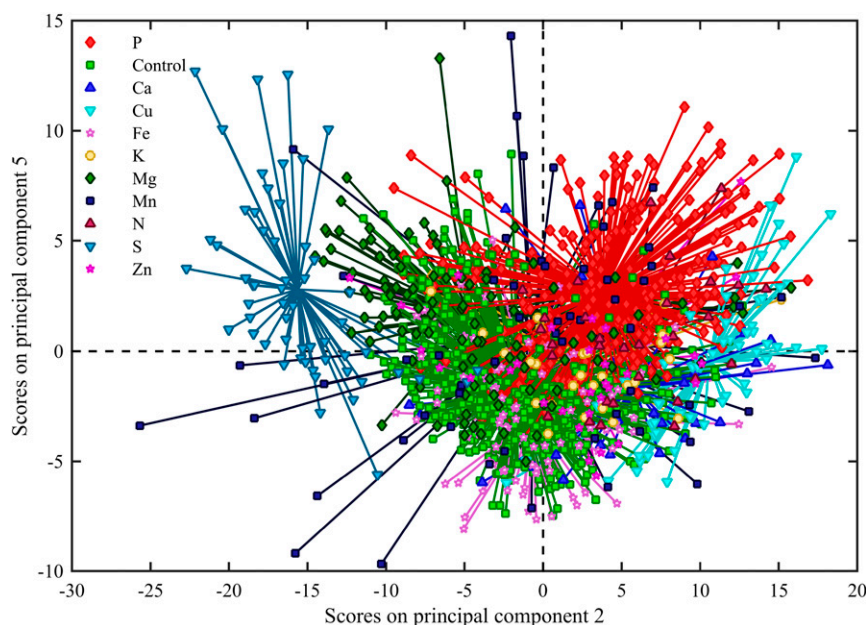


Figure 5. Score plot showing principal components 2 and 5 derived from a PCA analysis of OJIP transients from both barley and tomato plants with different nutrient deficiencies. Principal components 2 and 5 explained 10.0% and 2.6% of the variance, respectively. P-deficient samples clustered in the first quadrant. S-deficient samples are clustered in the second quadrant, and Cu-deficient samples are also seen to cluster on the border between the fourth and first quadrant.

cycle during dark adaptation (Schansker et al., 2005). Several enzymes of the Calvin cycle are known to be regulated by stromal orthophosphate and triose-P levels, ultimately influencing ATP and NADPH consumption (Rychter and Rao, 2009). Thus, it is conceivable that the I-P phase represents this final and slowest rate-limiting step of the photosynthetic electron transport chain and that it is modulated by the rate of NADPH consumption in the Calvin cycle. However, the primary mechanisms of P deficiency and the identity of the underlying processes reflected in the OJIP transient, particularly the I step, remain largely speculative (Schansker et al., 2011, 2014; Stirbet and Govindjee, 2012).

In this study, it was demonstrated that the effect of P deficiency was reversible when resupplying plants with P (Fig. 3; Supplemental Fig. S1), indicating that the disturbances to key processes were apparent and detectable before the photosynthetic apparatus had been permanently damaged. The unsupervised clustering of P-deficient tomato and barley plants in the PCA score plots (Fig. 5) highlights that a unique fingerprint of P deficiency was identified and that it was pertinent for both mono- and dicotyledonous species. The observed effect of P therefore appears to be associated with the electron transport of photosynthesis and thus constitutes a strong analytical tool to monitor the P status of higher plants in general.

Among the elements tested (N, P, K, Mg, Ca, S, Mn, Fe, Cu, and Zn), specific clustering was also observed for the elements S, Fe, Mg, Mn, and Cu (Fig. 5; Supplemental Fig. S5). S in particular shows a surprisingly clear grouping in the PCA plot (Fig. 5), which suggests that a unique fingerprint can also be identified for S deficiency in plants. Only a few studies have hitherto investigated the relationship between S deficiency and the resulting changes in chlorophyll *a* fluorescence transients. Antal et al. (2006) observed a striking suppression of the JIP phase in OJIP transients from S-deficient *Chlamydomonas reinhardtii*, similar to our observations (Supplemental Fig. S7). This was speculated to be caused by perturbations of both the donor and acceptor side of PSII, but no experimental evidence could be provided. In the classical work of Terry (1976), it was shown that the photosynthetic apparatus is a primary target of S deficiency and that it reduces photosynthesis via decreased levels of Rubisco activity, light-harvesting chlorophyll antenna, and ATP generation by photophosphorylation. Moreover, it has been shown that S deficiency affects electron transport between PSII and PSI and that it strongly impairs the ability of PSI to photoreduce NADP⁺ (Lunde et al., 2008). This is presumably done via a lower abundance of prominent electron carrier proteins such as cytochrome *b₆f* and ferredoxin as well as the PSI supercomplex. All these proteins share the common feature that they contain one or more Fe-S cofactors (Chitnis, 2001). This area, and the clustering likewise observed for Fe, Mg, Mn, and Cu (Fig. 5; Supplemental Fig. S5), represents obvious areas for future research.

Predicting the Bioactive P Concentration Using OJIP Transients and Chemometrics

To test the ability of OJIP transients to predict the P concentrations in leaf tissue, a PLS model was successfully generated. As indicated by the fitted cutoff value (Fig. 4b), it was possible to predict the P concentration of the barley YFDL up to the reported sufficiency level around 3,000 $\mu\text{g g}^{-1}$ DW (Reuter et al., 1997). Furthermore, for 92% of all validation samples, it was possible to correctly classify whether leaves contained above or below 2,000 $\mu\text{g P g}^{-1}$ DW. Field experiments suggest that this concentration constitutes a threshold for 30-d-old plants, leading to yield losses if no additional P fertilizer is added (Supplemental Table S3). The successful classification therefore shows that the technique is sufficiently sensitive to detect latent P deficiency before the yield potential is negatively affected, which allows for timely foliar P fertilization to correct the deficiency. Plants well supplied with P are known to store up to 85% to 95% of total P as a nonmetabolic pool in the cell vacuoles (Lauer et al., 1989). This explains the inability to predict P concentrations above the 3,000 $\mu\text{g g}^{-1}$ DW sufficiency level of the YFDL of barley plants. When P sufficiency has been reached, the metabolic processes reflected in the OJIP transients are saturated so that provision of additional P will have no effect. The OJIP transients are therefore effectively probing the bioactive P concentration in leaves.

The observed discrepancy between the fitted cutoff value around 3,000 $\mu\text{g P g}^{-1}$ DW and the inclusion of leaves with up to 3,600 $\mu\text{g g}^{-1}$ DW in the development of the PLS model reflects that there were a limited number of leaves with a concentration close to 3,000 $\mu\text{g P g}^{-1}$ DW in the calibration data set. It was therefore necessary to include leaves up to 3,600 $\mu\text{g g}^{-1}$ DW to get a sufficient representation of healthy P-sufficient leaves in the model.

Due to the simplicity of performing chlorophyll *a* fluorescence measurements, the observed specificity and successful prediction model demonstrate that OJIP transients can be used as a valuable probe to determine the bioactive P concentration of crops. This dynamic fluorescence analysis constitutes a strong tool for establishing unique site-specific P fertilization strategies based on timely measurements of the actual P status of the crop, thereby ensuring optimal yields while avoiding excessive use of natural P resources. Additionally, our results indicate that similar detection of other nutrient deficiencies might also be possible; future studies are thus needed to show whether multielement characterization of latent nutrient deficiency using chlorophyll *a* fluorescence is possible.

MATERIALS AND METHODS

Cultivation of Plants

Barley (*Hordeum vulgare* 'Quench') plants were cultivated in hydroponics (experiments 1, 2, and 4) or in soil (experiment 3) with different levels of P

availability. Barley seeds were pregerminated for 8 d (hydroponic experiments) or 4 d (soil experiment) in vermiculite in a greenhouse with minimum day/night temperatures of 18°C/15°C and a 16-h-day/8-h-night light regime. All nutrient solutions were prepared in Milli-Q water (Milli-Q Element). Control plants were supplied with a nutrient solution containing 200 μM KH_2PO_4 , 200 μM K_2SO_4 , 300 μM $\text{MgSO}_4 \cdot 7\text{H}_2\text{O}$, 100 μM NaCl , 300 μM $\text{Mg}(\text{NO}_3)_2 \cdot 6\text{H}_2\text{O}$, 900 μM $\text{Ca}(\text{NO}_3)_2 \cdot 4\text{H}_2\text{O}$, 600 μM KNO_3 , 50 μM $\text{Fe}(\text{III})\text{-EDTA-Na}$, 2 μM H_3BO_3 , 0.8 μM $\text{Na}_2\text{MoO}_4 \cdot 2\text{H}_2\text{O}$, 0.7 μM ZnCl_2 , 1.0 μM $\text{MnCl}_2 \cdot 4\text{H}_2\text{O}$, and 0.8 μM $\text{CuSO}_4 \cdot 5\text{H}_2\text{O}$. Different levels of P deficiency were induced, with hydroponically grown plants being supplied with combinations of the treatments P100, P50, P25, and P10 containing 89, 45, 22, and 9 μM KH_2PO_4 , respectively, to induce different P concentrations in the plants. A detailed description of the cultivation of the plants is included in Supplemental Text S1.

Measurements

Chlorophyll *a* Fluorescence

Chlorophyll *a* fluorescence transients (OJIP transients) were measured using a Handy PEA chlorophyll fluorometer (Hansatech Instruments). The midsection of the YFDL was dark adapted for at least 20 min before measuring, and a short, nonactinic light flash was used to adjust the gain of the detector. The actual measurement was conducted by illuminating the leaf with continuous actinic light at a saturating intensity ($>3,000 \mu\text{mol m}^{-2} \text{s}^{-1}$) for 10 s from three red LEDs, optically filtered to a maximum wavelength of 690 nm. The fluorescence transients were recorded using a PIN photodiode and a filter to ensure only wavelengths greater than 700 nm were recorded.

In experiment 1, measurements were performed on the YFDL 21 and 28 days after transplantation (DAT), giving 320 OJIP transients. In experiment 2, measurements were performed on the YFDL 21, 23, 28, and 30 DAT, giving 64 OJIP transients. Measurements on the second YFDL were also performed. In experiment 3, measurements were performed on the YFDL 3, 4, 5, and 6 weeks after transplanting, giving 120 OJIP transients. In experiment 4, measurements were performed on the YFDL 21, 28, and 31 DAT, giving a total of 200 OJIP transients. Measurements on the *Viridis-zb⁶³* mutant were performed 9 d after sowing (after 16 h of dark adaption); eight OJIP transients were obtained. To specifically reduce PSL, barley YFDLs from control and P25 treatments were harvested 21 DAT and illuminated for 60 s (720 nm; $30 \mu\text{mol m}^{-2} \text{s}^{-1}$) using a PAM-101 fluorometer connected with a near-infrared dual-E emitter and a dual-DR detector (Walz). Quickly hereafter, the clip was attached, and the OJIP transient was recorded as described above. The measurements were performed under green light.

To inoculate leaves with P, barley YFDLs from a P10 treatment were harvested 28 DAT and cut into three midleaf sections of 5 cm. The sections were immersed in 1 M KH_2PO_4 containing 0.2 mL L^{-1} Tween 20 for 30, 60, or 120 min (four leaf sections in each treatment). After inoculation, the leaves were wiped, a clip was attached and dark adapted for 20 min in a zip bag, and the OJIP transient was recorded. As a control, leaves from the same P10 treatment were immersed in Milli-Q water with 0.2 mL L^{-1} Tween.

Chlorophyll, Carotenoid, and Anthocyanin Concentration

Concentrations of chlorophylls and carotenoids were determined in leaf material from the midsection of the YFDL as described by Lichtenthaler and Wellburn (1983) using methanol and determined by UV-Vis spectroscopy (Genesys 10S, Thermo Scientific). Determination of anthocyanin concentrations was performed according to the method described by Ticconi et al. (2001) using the same leaf material as described above. An EON microplate spectrophotometer (BioTek Instruments) was used to measure the absorbance at 535 and 650 nm and calculate the anthocyanin concentration.

Element Analysis

Leaf concentrations of P, Fe, Mg, Mn, Zn, K, S, and Ca were determined using inductively coupled plasma-optical emission spectroscopy (Optima 5300DV, PerkinElmer) following the procedure described in Laursen et al. (2011) and Hansen et al. (2009). YFDLs from experiment 1 were freeze dried and grounded in zirconium-coated jars containing a zirconium-coated ball in a ball mill (MM301, Retsch), whereas YFDLs from experiments 2, 3, and 4 and the field experiment were oven dried at 50°C until completely dry. Data quality was evaluated by including at least five samples of digested, certified reference material (NIST 1515, apple [*Malus* spp.] leaf, National Institute of Standards and Technology) in each analytical run. Data were processed using the WinLab32 software (version 3.1.0.0107; PerkinElmer).

Chemometric Analysis

Data were analyzed by the chemometric methods PCA (Martens and Næs, 1989) and PLS (Wold et al., 2001), carried out using Matlab R2015a (Mathworks) and PLS_Toolbox 7.9 (Eigenvector Research).

Preprocessing

As the observed effect of P deficiency affected the second and higher order components, all OJIP transients were normalized by F_0 and subtracted by 1 to have origin at 0. The resulting fluorescence transients were then first-order corrected to minimize lower order variations by a method similar to multiplicative scatter correction and standard normal variate preprocessing (Geladi et al., 1985; Helland et al., 1995). This adjusted the overall offset and slope of all transients, yet did not affect the second and higher order components of the curves. All OJIP transients were subsequently differentiated, scaled, and smoothed using a Savitzky-Golay filter (Savitzky and Golay, 1964). For more details, see Supplemental Text S1.

For the PCA, the full data set used for the analysis was additionally mean centered to emphasize variations from the mean OJIP transient over the included data set of transients from both this experiment and previous experiments (Hebborn et al., 2009; Husted et al., 2009; Schmidt et al., 2013). Leaves with a P concentration above 3,000 $\mu\text{g g}^{-1}$ DW were marked as healthy control leaves, and leaves with a P concentration below 2,000 $\mu\text{g g}^{-1}$ DW were marked as P deficient. Leaves between these boundaries (2,000–3,000 $\mu\text{g g}^{-1}$ DW) were not included in this particular analysis.

Outlier Detection

Data outliers were detected based on interpretations of score plots of the principal components included in the PCA and PLS analyses as well as plots showing the Q residuals and Hotelling T^2 (Hotelling, 1931) parameters for each transient.

One hundred fifty-nine OJIP transients from 38 independent growth units were included in the calibration data set. Two hundred ninety-one of 382 OJIP transients were included in the validation data set. In the PCA, 35 OJIP transients were removed as outliers, leaving a data set of 1,228 OJIP transients. For more details, see Supplemental Text S1.

Supplemental Data

The following supplemental materials are available.

Supplemental Figure S1. Temporal evolution of P-resupplied leaf.

Supplemental Figure S2. Effects on OJIP transients.

Supplemental Figure S3. Fluorescence rate of change.

Supplemental Figure S4. PLS regression vector.

Supplemental Figure S5. PCA scores plots.

Supplemental Figure S6. PCA loadings.

Supplemental Figure S7. OJIP transients from Cu-, S-, and P-deficient plants.

Supplemental Table S1. Inductively Coupled Plasma-Mass Spectrometry elemental analysis results.

Supplemental Table S2. Harvest data.

Supplemental Table S3. Field trial data.

Supplemental Text S1. Additional information.

ACKNOWLEDGMENTS

We thank Lena Byrgesen and Thomas H. Hansen for assistance with the multielement inductively coupled plasma-optical emission spectroscopy analyses. Received June 2, 2015; accepted July 7, 2015; published July 10, 2015.

LITERATURE CITED

- Antal T, Rubin A** (2008) In vivo analysis of chlorophyll *a* fluorescence induction. *Photosynth Res* 96: 217–226
Antal TK, Volgusheva AA, Kukarskih GP, Bulychev AA, Krendeleva TE, Rubin AB (2006) Effects of sulfur limitation on photosystem II

- functioning in *Chlamydomonas reinhardtii* as probed by chlorophyll *a* fluorescence. *Physiol Plant* **128**: 360–367
- Chitnis PR** (2001) PHOTOSYSTEM I: function and physiology. *Annu Rev Plant Physiol Plant Mol Biol* **52**: 593–626
- Cordell D, Drangert JO, White S** (2009) The story of phosphorus: global food security and food for thought. *Glob Environ Change* **19**: 292–305
- Edixhoven JD, Gupta J, Savenije HHG** (2013) Recent revisions of phosphate rock reserves and resources: reassuring or misleading? An in-depth literature review of global estimates of phosphate rock reserves and resources. *Earth System Dynamics Discussions* **4**: 1005–1034
- Elsler J, Bennett E** (2011) Phosphorus cycle: a broken biogeochemical cycle. *Nature* **478**: 29–31
- Engels C, Kirkby E, White P** (2012) Mineral nutrition, yield and source: sink relationships. In P Marschner, ed, *Marschner's Mineral Nutrition of Higher Plants*. Elsevier, London, pp 85–133
- Foley JA, Ramankutty N, Brauman KA, Cassidy ES, Gerber JS, Johnston M, Mueller ND, O'Connell C, Ray DK, West PC, et al** (2011) Solutions for a cultivated planet. *Nature* **478**: 337–342
- Food and Agriculture Organization of the United Nations** (2009) Feeding the world, eradicating hunger. http://www.fao.org/fileadmin/templates/wsfs/Summit/WSFS_Issues_papers/WSFS_Background_paper_Feeding_the_world.pdf (June 24, 2015)
- Geladi P, MacDougall D, Martens H** (1985) Linearization and scatter-correction for near-infrared reflectance spectra of meat. *Appl Spectrosc* **39**: 491–500
- Gilbert N** (2009) Environment: the disappearing nutrient. *Nature* **461**: 716–718
- Godfray HCJ, Beddington JR, Crute IR, Haddad L, Lawrence D, Muir JF, Pretty J, Robinson S, Thomas SM, Toulmin C** (2010) Food security: the challenge of feeding 9 billion people. *Science* **327**: 812–818
- Govindjee** (2004) Chlorophyll *a* fluorescence: a bit of basics and history. In GC Papageorgiou, Govindjee, eds, *Chlorophyll *a* Fluorescence: A Signature of Photosynthesis*. Springer, Dordrecht, The Netherlands, pp 1–41
- Hansen TH, Laursen KH, Persson DP, Pedas P, Husted S, Schjoerring JK** (2009) Micro-scaled high-throughput digestion of plant tissue samples for multi-elemental analysis. *Plant Methods* **5**: 12
- Harbinson J, Rosenqvist E** (2003) An introduction to chlorophyll fluorescence. In *Practical Applications of Chlorophyll Fluorescence in Plant Biology*. Springer, Boston, MA, pp 1–29
- Hawkesford M, Horst W, Kichey T, Lambers H, Schjoerring J, Møller IS, White P** (2012) Functions of macronutrients. In P Marschner, ed, *Marschner's Mineral Nutrition of Higher Plants*. Elsevier, London, pp 135–189
- Hebbern CA, Laursen KH, Ladegaard AH, Schmidt SB, Pedas P, Bruhn D, Schjoerring JK, Wulfsohn D, Husted S** (2009) Latent manganese deficiency increases transpiration in barley (*Hordeum vulgare*). *Physiol Plant* **135**: 307–316
- Helland IS, Næs T, Isaksson T** (1995) Related versions of the multiplicative scatter correction method for preprocessing spectroscopic data. *Chemom Intell Lab Syst* **29**: 233–241
- Hernández I, Munné-Bosch S** (2015) Linking phosphorus availability with photo-oxidative stress in plants. *J Exp Bot* **66**: 2889–2900
- Hotelling H** (1931) The generalization of student's ratio. *Ann Math Stat* **2**: 360–378
- Husted S, Laursen KH, Hebbern CA, Schmidt SB, Pedas P, Haldrup A, Jensen PE** (2009) Manganese deficiency leads to genotype-specific changes in fluorescence induction kinetics and state transitions. *Plant Physiol* **150**: 825–833
- Jiang HX, Tang N, Zheng JG, Li Y, Chen LS** (2009) Phosphorus alleviates aluminum-induced inhibition of growth and photosynthesis in *Citrus grandis* seedlings. *Physiol Plant* **137**: 298–311
- Joly D, Carpentier R** (2007) The oxidation/reduction kinetics of the plastoquinone pool controls the appearance of the I-peak in the O–J–I–P chlorophyll fluorescence rise: effects of various electron acceptors. *J Photochem Photobiol B* **88**: 43–50
- Joly D, Jemâa E, Carpentier R** (2010) Redox state of the photosynthetic electron transport chain in wild-type and mutant leaves of *Arabidopsis thaliana*: impact on photosystem II fluorescence. *J Photochem Photobiol B* **98**: 180–187
- Kastori R, Plesnicar M, Arsenijevic-Maksimovic I, Petrovic N, Pankovic D, Sakac Z** (2000) Photosynthesis, chlorophyll fluorescence, and water relations in young sugar beet plants as affected by sulfur supply. *J Plant Nutr* **23**: 1037–1049
- Kautsky H, Hirsch A** (1931) Neue versuche zur kohlen säureassimilation. *Naturwissenschaften* **19**: 964
- Laisk A, Eichelmann H, Oja V** (2009) Leaf C3 photosynthesis in silico: integrated carbon/nitrogen metabolism. In A Laisk, L Nedbal, Govindjee, eds, *Photosynthesis in Silico*. Springer Netherlands, Dordrecht, The Netherlands, pp 295–322
- Larbi A, Abadía A, Morales F, Abadía J** (2004) Fe resupply to Fe-deficient sugar beet plants leads to rapid changes in the violaxanthin cycle and other photosynthetic characteristics without significant de novo chlorophyll synthesis. *Photosynth Res* **79**: 59–69
- Lauer MJ, Blevins DG, Sierzputowska-Gracz H** (1989) P-nuclear magnetic resonance determination of phosphate compartmentation in leaves of reproductive soybeans (*Glycine max* L.) as affected by phosphate nutrition. *Plant Physiol* **89**: 1331–1336
- Laursen KH, Schjoerring JK, Olesen JE, Askegaard M, Halekoh U, Husted S** (2011) Multielemental fingerprinting as a tool for authentication of organic wheat, barley, faba bean, and potato. *J Agric Food Chem* **59**: 4385–4396
- Lichtenthaler HK, Wellburn AR** (1983) Determinations of total carotenoids and chlorophylls *b* of leaf extracts in different solvents. *Biochem Soc Trans* **11**: 591–592
- Lin ZH, Chen LS, Chen RB, Zhang FZ, Jiang HX, Tang N** (2009) CO₂ assimilation, ribulose-1,5-bisphosphate carboxylase/oxygenase, carbohydrates and photosynthetic electron transport probed by the JIP-test, of tea leaves in response to phosphorus supply. *BMC Plant Biol* **9**: 43
- Lunde C, Zygadlo A, Simonsen HT, Nielsen PL, Blennow A, Haldrup A** (2008) Sulfur starvation in rice: the effect on photosynthesis, carbohydrate metabolism, and oxidative stress protective pathways. *Physiol Plant* **134**: 508–521
- MacDonald GK, Bennett EM, Potter PA, Ramankutty N** (2011) Agronomic phosphorus imbalances across the world's croplands. *Proc Natl Acad Sci USA* **108**: 3086–3091
- Mallick N, Mohn FH** (2003) Use of chlorophyll fluorescence in metal-stress research: a case study with the green microalga *Scenedesmus*. *Ecotoxicol Environ Saf* **55**: 64–69
- Martens H, Næs T** (1989) *Multivariate Calibration*. John Wiley & Sons Chichester, UK
- McAlister ED, Myers J** (1940) *The Time Course Of Photosynthesis and Fluorescence Observed Simultaneously*. Smithsonian Miscellaneous Collections, Washington, DC
- Nielsen VS, Scheller HV, Møller BL** (1996) The photosystem I mutant viridis-zb63 of barley (*Hordeum vulgare*) contains low amounts of active but unstable photosystem I. *Physiol Plant* **98**: 637–644
- Obersteiner M, Peñuelas J, Ciais P, van der Velde M, Janssens IA** (2013) The phosphorus trilemma. *Nat Geosci* **6**: 897–898
- Pospisil P, Dau H** (2002) Valinomycin sensitivity proves that light-induced thylakoid voltages result in millisecond phase of chlorophyll fluorescence transients. *Biochim Biophys Acta* **1554**: 94–100
- Reuter DJ, Robinson JB, Dutkiewicz C** (1997) *Plant Analysis: An Interpretation Manual*, Ed 2. CSIRO Publishing, Collingwood, Australia
- Ripley BS, Redfern SP, Dames JF** (2004) Quantification of the photosynthetic performance of phosphorus-deficient *Sorghum* by means of chlorophyll-*a* fluorescence kinetics. *S Afr J Sci* **100**: 615–618
- Rychter A, Rao I** (2009) Role of phosphorus in photosynthetic carbon metabolism. In M Pessaraki, ed, *Handbook of Photosynthesis*, Ed 2. Taylor & Francis, Boca Raton, FL, pp 123–148
- Savitzky A, Golay MJE** (1964) Smoothing and differentiation of data by simplified least squares procedures. *Anal Chem* **36**: 1627–1639
- Schansker G, Tóth SZ, Holzwarth AR, Garab G** (2014) Chlorophyll *a* fluorescence: beyond the limits of the Q_A model. *Photosynth Res* **120**: 43–58
- Schansker G, Tóth SZ, Kovács L, Holzwarth AR, Garab G** (2011) Evidence for a fluorescence yield change driven by a light-induced conformational change within photosystem II during the fast chlorophyll *a* fluorescence rise. *Biochim Biophys Acta* **1807**: 1032–1043
- Schansker G, Tóth SZ, Strasser RJ** (2005) Methylviologen and dibromothymoquinone treatments of pea leaves reveal the role of photosystem I in the Chl *a* fluorescence rise OJIP. *Biochim Biophys Acta* **1706**: 250–261
- Schmidt SB, Pedas P, Laursen KH, Schjoerring JK** (2013) Latent manganese deficiency in barley can be diagnosed and remediated on the basis of chlorophyll *a* fluorescence measurements. *Plant Soil* **372**: 417–429

- Schröder JJ, Smit AL, Cordell D, Rosemarin A** (2011) Improved phosphorus use efficiency in agriculture: a key requirement for its sustainable use. *Chemosphere* **84**: 822–831
- Stirbet A, Govindjee** (2011) On the relation between the Kautsky effect (chlorophyll *a* fluorescence induction) and photosystem II: basics and applications of the OJIP fluorescence transient. *J Photochem Photobiol B* **104**: 236–257
- Stirbet A, Govindjee** (2012) Chlorophyll *a* fluorescence induction: a personal perspective of the thermal phase, the J-I-P rise. *Photosynth Res* **113**: 15–61
- Tang N, Li Y, Chen LS** (2012) Magnesium deficiency-induced impairment of photosynthesis in leaves of fruiting *Citrus reticulata* trees accompanied by up-regulation of antioxidant metabolism to avoid photo-oxidative damage. *J Plant Nutr Soil Sci* **175**: 784–793
- Terry N** (1976) Effects of sulfur on the photosynthesis of intact leaves and isolated chloroplasts of sugar beets. *Plant Physiol* **57**: 477–479
- Ticconi CA, Delatorre CA, Abel S** (2001) Attenuation of phosphate starvation responses by phosphite in *Arabidopsis*. *Plant Physiol* **127**: 963–972
- Veneklaas EJ, Lambers H, Bragg J, Finnegan PM, Lovelock CE, Plaxton WC, Price CA, Scheible WR, Shane MW, White PJ, et al** (2012) Opportunities for improving phosphorus-use efficiency in crop plants. *New Phytol* **195**: 306–320
- Weng XY, Xu HX, Yang Y, Peng HH** (2008) Water-water cycle involved in dissipation of excess photon energy in phosphorus deficient rice leaves. *Biol Plant* **52**: 307–313
- Wold S, Sjöström M, Eriksson L** (2001) PLS-regression: a basic tool of chemometrics. *Chemom Intell Lab Syst* **58**: 109–130
- Yang GH, Yang LT, Jiang HX, Li Y, Wang P, Chen LS** (2012) Physiological impacts of magnesium-deficiency in *Citrus* seedlings: photosynthesis, antioxidant system and carbohydrates. *Trees (Berl)* **26**: 1237–1250

1 **Supplementary Information**

2 **Cultivation of plants**

3 **Experiment 1: Induction of gradual phosphorus deficiency in hydroponic plants** 4 **(calibration set)**

5 Barley seedlings were transferred to 32 black 4L containers filled with nutrients dissolved in
6 double deionized water. Nutrient solutions were changed weekly and aerated using steel medical
7 syringes. Each container held ten plants fitted in a lid. In all containers, pH was kept constant at
8 6.0 ± 0.3 using ultrapure HCl. Plants were cultivated in two growth chambers at a 16/8 h
9 day/night light regime under normal light settings ($400 \mu\text{mol photons m}^{-2} \text{s}^{-1}$) and a constant
10 temperature (20°C). Ten days after transplanting (DAT) the plants were divided into two groups,
11 either maintained under the above-mentioned conditions or exposed to an increased light
12 intensity ($750 \mu\text{mol photons m}^{-2} \text{s}^{-1}$), and a decreased temperature (15°C). The position of all
13 containers was randomized frequently within each climate chamber to avoid any systematic
14 effects. The 16 units in each growth chamber were further divided into four different P
15 treatments including control, P100, P50 and P10. The control nutrient solution contained $200 \mu\text{M}$
16 KH_2PO_4 , $200 \mu\text{M}$ K_2SO_4 , $300 \mu\text{M}$ $\text{MgSO}_4 \cdot 7 \text{H}_2\text{O}$, $100 \mu\text{M}$ NaCl , $300 \mu\text{M}$ $\text{Mg}(\text{NO}_3)_2 \cdot 6 \text{H}_2\text{O}$, 900
17 μM $\text{Ca}(\text{NO}_3)_2 \cdot 4 \text{H}_2\text{O}$, $600 \mu\text{M}$ KNO_3 , $50 \mu\text{M}$ $\text{Fe}(\text{III})\text{-EDTA-Na}$, $2.0 \mu\text{M}$ H_3BO_3 , $0.8 \mu\text{M}$
18 $\text{Na}_2\text{MoO}_4 \cdot 2 \text{H}_2\text{O}$, $0.7 \mu\text{M}$ ZnCl_2 , $1.0 \mu\text{M}$ $\text{MnCl}_2 \cdot 4 \text{H}_2\text{O}$ and $0.8 \mu\text{M}$ $\text{CuSO}_4 \cdot 5 \text{H}_2\text{O}$. During the
19 first week after transplanting the concentration of micronutrients was however reduced by 50%
20 in order to avoid EDTA poisoning of the young plants. Initially (<10 DAT), P100, P50 and P10
21 plants were all supplied with $89 \mu\text{M}$ KH_2PO_4 to ensure sufficient P supply, while avoiding
22 luxury uptake. In the following period, the KH_2PO_4 concentration was reduced to $45 \mu\text{M}$ and 9
23 μM for P50 and P10 treatments, respectively. Twelve days after induction of P50 and P10
24 treatments, *i.e.* 22 DAT, P100, P50 and P10 treatments were deprived completely of P for the
25 rest of the experimental period.

26 **Experiment 2: Induction of gradual phosphorus deficiency in hydroponic plants (validation** 27 **set)**

28 The experiment was carried out in a greenhouse under the same climatic conditions as for pre-
29 germination of seeds. 16 hydroponic 4L containers were used, each with four barley plants fitted
30 in the lid. Each container was aerated, the pH kept at 6.0 ± 0.3 , and nutrient solution changed
31 weekly similar to experiment 1. The first 10 DAT, all containers were provided control nutrient
32 solution similar to experiment 1. Then four P treatments were induced, control, P100, P50 and
33 P25, each applied to four cultivation units. P100 and P50 treatments were similar to P100 and
34 P50 in experiment 1, whereas P25 treated plants received $22 \mu\text{M}$ KH_2PO_4 . Furthermore, KCl
35 was added to ensure a constant potassium concentration for all treatments, depending on the
36 added amount of KH_2PO_4 . 21 DAT, P was completely removed from P100, P50 and P25

37 treatments. At 28 DAT, P was resupplied by providing all containers with control nutrient
38 solution.

39 **Experiment 3: Induction of phosphorus deficiency in soil cultivated plants (validation set)**

40 Experiment 3 was carried out in a greenhouse under the same climatic conditions as experiment
41 2. The experimental setup consisted of 30 pots, each holding 4.5 kg soil, divided into 6 different
42 treatments (+P, W3, W4, W5, W6 and -P). The soil was sampled (0-25 cm) from a known P
43 deficient field (sandy loam: Clay 16%, silt 17% and sand 67%, located at University of
44 Copenhagen experimental field station, 55° 40' N, 12° 17' E), air-dried and sieved through an 8
45 mm sieve. All soil received a basic fertilizer containing N (21.5 %), K (10.6 %), S (3.6 %), Mg
46 (1.0 %) and B (0.02 %) at a rate equivalent to 300 mg N kg⁻¹. The soil for the control treatment
47 (+P) was furthermore fertilized with triple super phosphate (20 % P) at a rate of 0.2 g P kg⁻¹ soil
48 prior to plant growth. After pre-germination, nine barley plants were transferred into each pot.
49 Four days later, this was reduced to seven plants. Three weeks after transplanting, W3 treated
50 pots received triple super phosphate in the same amount as for the control treatment, by
51 sprinkling the fertilizer on the soil surface. This procedure was repeated in week 4, 5 and 6 after
52 transplanting (treatment W4, W5, and W6, respectively). The last treatment (-P) did not receive
53 any P fertilizer. The soil was kept moist throughout the experiment by irrigation with Milli-Q
54 water from the top.

55 **Experiment 4: Induction of gradual phosphorus deficiency in hydroponic plants (validation 56 set)**

57 Experiment 4 was carried out in a greenhouse under the same climatic conditions as for
58 experiment 2. 25 hydroponic 4L containers were used, each with four barley plants fitted in the
59 lid. Each container was aerated, the pH kept at 6.0 ± 0.3, and nutrient solution changed weekly
60 similar to experiment 1 and 2. Five containers were provided control nutrient solution, while the
61 remaining 20 containers were provided with P100 solution (89 μM KH₂PO₄). 10 DAT, three
62 treatments were induced from 15 containers initially provided with P100. 3×5 containers each
63 received 45 μM, 22 μM and 9 μM KH₂PO₄ (P50, P25, and P10), respectively. KCl was added
64 correspondingly as in experiment 2. 21 DAT one plant from each cultivation unit was harvested,
65 and P was completely removed from treatments P100, P50, P25 and P10. Other provided
66 nutrients were accordingly reduced to ¾ of the original concentration to account for the
67 harvested plant. At 28 DAT, two plants from each cultivation unit were harvested, and all
68 containers we provided with the control nutrient solution, adjusted accordingly to supply only
69 one plant in each unit.

70 ***Viridis-zb*⁶³ – Barley photosystem I mutant**

71 Seeds from the barley-mutant *Viridis-zb*⁶³ were cultivated in vermiculite in a climate chamber
72 with short day settings (8/16 hours day/night light regime under low light settings (150 μmol
73 photons m⁻² s⁻¹) and a constant temperature at 20°C). After eight days, the plants were moved for
74 darkadaption for 16 hours. The plants did only receive Milli-Q water during the experiment.

75 **Field experiments**

76 Based on low P availability, 16 locations in Denmark were selected for field trials in the summer
77 of 2013 and 2014. At each location, 8 plots of 60 m² were placed in a randomized experiment.
78 The entire experiment received a basic fertilizer containing N (21.5 %), K (10.6 %), S (3.6 %),
79 Mg (1.0 %) and B (0.02 %) in amounts corresponding to 110 kg N ha⁻¹. At sowing, 4 plots
80 received triple superphosphate in amounts corresponding to 30 kg P ha⁻¹ placed below the seeds,
81 while the remaining 4 plots received no P fertilizer throughout the growing season. All plots
82 were sown with spring barley (*Hordeum vulgare* L. cv. Quench), drilled with 300 seeds m⁻², and
83 the YFDL was collected 30 days after sowing. At full maturity, 10–30 m² from each plot were
84 harvested and grain yields were recorded. Statistical analysis on grain yields was performed
85 using the Data Analysis add-in in Microsoft Excel 2010 (Microsoft Corporation, Redmond,
86 Washington, USA).

87 **Historical data**

88 OJIP transients from a range of previously conducted experiments (Hebbern et al., 2009; Husted
89 et al., 2009; Schmidt et al., 2013) were collected to validate the specificity of the observed effect
90 on OJIP transients from P deficient plants. The transients were measured on barley (*Hordeum*
91 *vulgare* L.) and tomato (*Solanum lycopersicum* L.) plants, which were cultivated in hydroponics
92 under greenhouse conditions comparable to those in experiment 2 and 3. Different nutrient
93 deficiencies (N, P, K, Ca, S, Mg, Fe, Cu, Zn and B) were induced by removing the single
94 element from the control nutrient solution noted for experiment 1. OJIP transients were collected
95 at a time when nutrient deficiencies were expected to be apparent in the plants.

96 **Chemometric analysis**

97 PCA is an unsupervised method that enables a simple and comprehensive overview of the major
98 variations in a multivariate data set by reducing the number of dimensions with a minor loss of
99 information. Data is presented using the principal components (PC's) as axes, PC 1 explains the
100 most variance in the dataset, and subsequent PC's explain continuously less variance until only
101 noise and/or single sample effects are represented by higher PC's. PCA is described more
102 thoroughly in *e.g.* Martens and Næs, 1989.

103 PLS analysis is related to PCA. However, in PLS the new sets of principal components are
104 determined to maximize the covariance between measurements (X) and a corresponding set of
105 reference data, Y. The resulting model can be used for prediction of Y-values using new X-data
106 as input. The method is further described in *e.g.* Wold et al., 2001.

107 **Preprocessing**

108 Before PCA and PLS analysis, the OJIP transients were preprocessed. The measured transients
109 displayed unwanted variations both within and between individual experiments. These variations
110 included differences in the maximum fluorescence, the overall slope and offset of the transients
111 due to both the nature of the fluorescence measurements and the spectroscopic hardware used,
112 which adjusts detector gain and offset for each individual measurement. As the observed effect
113 of P deficiency affected the second and higher order components of the OJIP transients, all OJIP

114 transients were initially normalized by F_0 and subtracted by one to have an origin at zero. The
115 resulting $F(t)/F_0$ transients were then first-order-corrected to further minimize lower order
116 variations within and between experiments. This was achieved by calculating an offset- and
117 multiplicative factor to each individual transient that minimized the difference to the median of
118 the transients from the control plants in the calibration dataset. This effectively adjusted the
119 overall offset and slope of all transients and thus made them more comparable, yet did not affect
120 the second and higher order components of the curves. Mathematically this resembles MSC or
121 SNV preprocessing (Geladi et al., 1985; Helland et al., 1995). All OJIP transients were
122 subsequently differentiated by dividing the change in fluorescence with the difference in time
123 between successive data points. To emphasize the features of the I-P phase of the transient, the
124 differentiated curve were scaled by a composite exponential function designed to enhance the I-
125 step of the OJIP transient and subsequently smoothed using a Savitzky-Golay filter (Savitzky
126 and Golay, 1964), fitting a second order polynomial to a moving window of 15 neighbouring
127 data points.

128 For the PCA, the full dataset used for the analysis was additionally mean centered to emphasize
129 variations from the mean OJIP transient over the included dataset of transients from both the
130 current and previous experiments (Hebberner et al., 2009; Husted et al., 2009; Schmidt et al.,
131 2013). From experiments 1-4, leaves with a P concentration above $3000 \mu\text{g g}^{-1}$ DW were marked
132 as healthy control leaves, and leaves with a P concentration below $2000 \mu\text{g g}^{-1}$ DW were marked
133 as P deficient. Leaves between these boundaries ($2000\text{-}3000 \mu\text{g g}^{-1}$ DW) were not included in
134 this particular analysis.

135 For the PLS analysis, OJIP transients from experiment 1 were used as calibration dataset, and
136 OJIP transients from experiment 2, 3 and 4 were used as validation dataset. Leaves from the
137 same growth unit were pooled in experiment 1, and therefore groups of 5 OJIP transients shared
138 the same reference value. Due to variations between plants in the same growth unit, some of
139 these groups of 5 were poorly represented by one common reference value. For this reason, the
140 root mean squared error (RMSE) for individual transients to the median of the group was
141 calculated, along with the median average deviation (MAD) between the sum of fluorescence
142 intensity around the I-step for the 5 transients in a group. The top 10 percentile of the individual
143 OJIP transients with highest RMSE-values, and the top 15 percentile of the groups of OJIP
144 transients with the highest MAD-values were not included in the PLS analysis as these were not
145 well described by the single reference value associated with them. In experiment 4, the reference
146 value for the plant harvested 21 DAT was used as reference value for all four OJIP transients
147 measured from the four plants in that growth unit. 28 DAT, a specific reference value was
148 measured for two of the remaining three plants; the measurement on the last plant was assigned
149 the mean reference value of the two harvested plants. 31 DAT, a specific reference value was
150 obtained for the OJIP transient from the single remaining plant in each growth unit.

151 **Outlier detection**

152 Data outliers were detected based on interpretations of score plots of the principal components
153 included in the PCA and PLS analyses, as well as plots showing the Q residuals and Hotelling T^2
154 parameters for each transient. Q residuals represent the residual between the actual transient and

155 its projection in the principal components of the model; a high Q residual therefor reflects a poor
156 fit in the model. Hotelling T^2 values arises as a generalization of Student's t-distribution
157 (Hotelling, 1931), and a high Hotelling T^2 value reflects a sample that has a high leverage in the
158 model. In these plots, outliers are defined as transients that differ significantly from the majority
159 of the samples; i.e. transients that plot very separate from other transients in score plots, or
160 transients with very high Q residual or Hotelling T^2 values.

161 159 OJIP transients from 38 independent growth units were included in the calibration dataset.
162 Thus, 161 OJIP transients out of 320 total OJIP transients were not included in the development
163 of the PLS model due to the foliar P concentration of the measured leaves being outside the
164 included 0-3600 $\mu\text{g P g}^{-1}$ DW range, or because they were data outliers. 291 of 382 OJIP
165 transients were included in the validation dataset; the excluded samples were identified as data
166 outliers. For the PCA, 35 OJIP transients were removed from the analysis as outliers, leaving a
167 total of 1228 OJIP transients in the analysis.

168

169 **References**

170 Geladi P, MacDougall D, Martens H (1985) Linearization and Scatter-Correction for Near-Infrared Reflectance Spectra of Meat.
171 *Applied Spectroscopy* 39: 491–500

172 Hebborn CA, Laursen KH, Ladegaard AH, Schmidt SB, Pedas P, Bruhn D, Schjoerring JK, Wulfsohn D, Husted S (2009) Latent
173 manganese deficiency increases transpiration in barley (*Hordeum vulgare*). *Physiologia Plantarum* 135: 307–316

174 Helland IS, Næs T, Isaksson T (1995) Related versions of the multiplicative scatter correction method for preprocessing
175 spectroscopic data. *Chemometrics and Intelligent Laboratory Systems* 29: 233–241

176 Hotelling H (1931) The Generalization of Student's Ratio. *Ann Math Statist* 2: 360–378

177 Husted S, Laursen KH, Hebborn CA, Schmidt SB, Pedas P, Haldrup A, Jensen PE (2009) Manganese Deficiency Leads to
178 Genotype-Specific Changes in Fluorescence Induction Kinetics and State Transitions. *Plant Physiol* 150: 825–833

179 Martens H, Næs T (1989) *Multivariate Calibration*. John Wiley & Sons

180 Savitzky A, Golay MJE (1964) Smoothing and Differentiation of Data by Simplified Least Squares Procedures. *Analytical*
181 *chemistry* 36: 1627–1639

182 Schmidt SB, Pedas P, Laursen KH, Schjoerring JK (2013) Latent manganese deficiency in barley can be diagnosed and
183 remediated on the basis of chlorophyll a fluorescence measurements. *Plant Soil* 372: 417–429

184 Wold S, Sjöström M, Eriksson L (2001) PLS-regression: a basic tool of chemometrics. *Chemometrics and Intelligent Laboratory*
185 *Systems* 58: 109–130

186

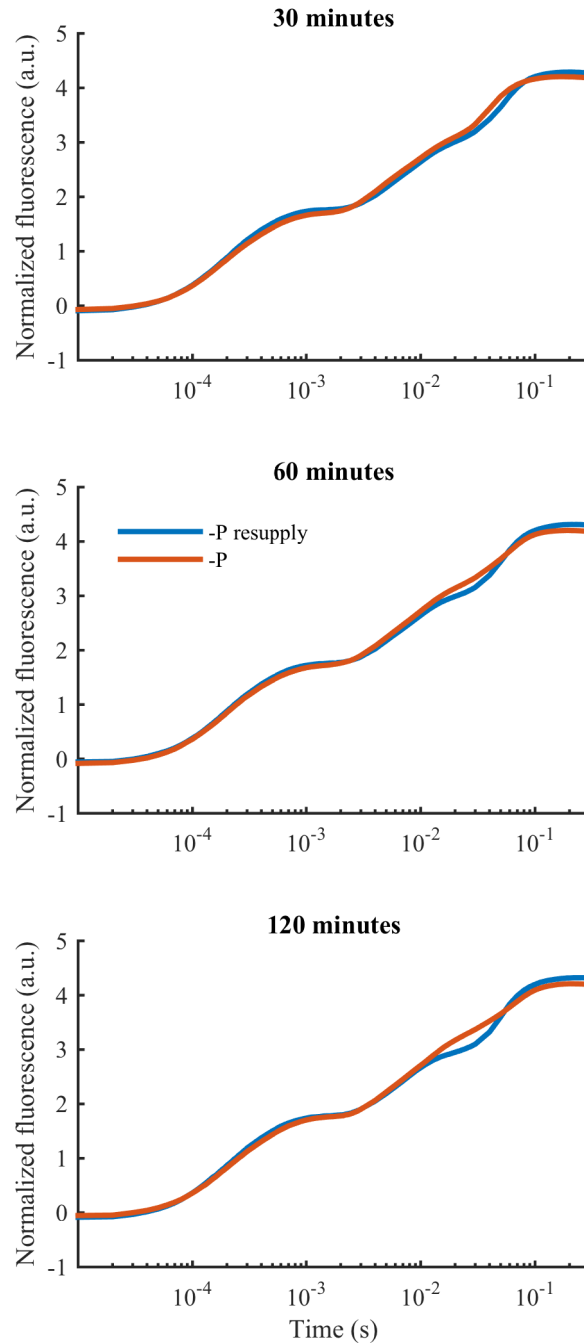


Figure S1: OJIP transient of a P deficient barley leaf resupplied with P (-P resupply), and the OJIP transient of a P deficient barley leaf kept in Milli-Q water (-P) after 30, 60 and 120 minutes. It is seen how the I-step is beginning to re-emerge already after 30 minutes, has grown stronger after 60 minutes and appear fully re-established after 120 minutes.

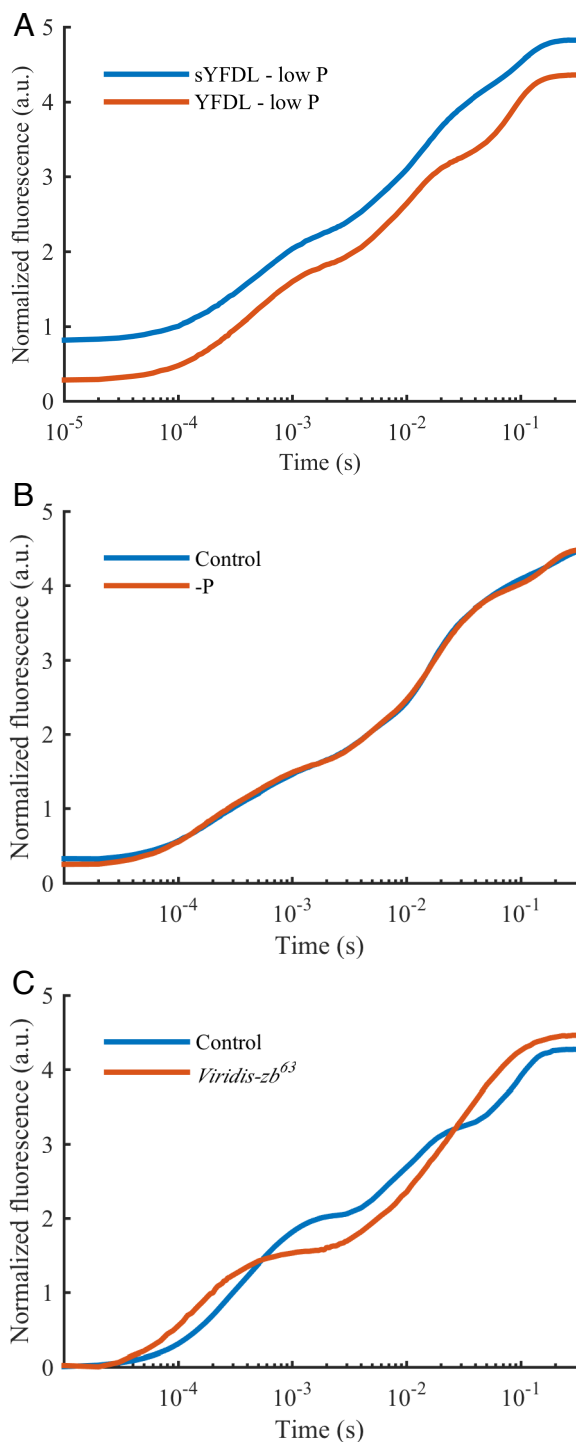


Figure S2: OJIP transients probing aspects of the observed effect of P deficiency **A)** OJIP transients from the youngest fully developed leaf (YFDL) and second youngest fully developed leaf (sYFDL) from a barley plant grown under P deficient conditions (YFDL = $1200 \mu\text{g P g}^{-1} \text{ DW}$) 21 days after transplantation. It is evident that while the I-step is still visible in the moderately P deficient YFDL, it has straightened completely in the sYFDL. The sYFDL transient has been offset by 1 arbitrary unit (a.u.) to improve legibility. **B)** The OJIP transients from a healthy control and a P deficient barley plant, when illuminated for 60 seconds with far red light to reduce PSI prior to measuring the OJIP transient. The difference observed between the control and P deficient plants under standard measuring conditions has been completely eliminated. **C)** OJIP transient measured on a *Viridis-zb63* mutant compared to a OJIP transient measured from a healthy control plant in experiment 1. Due to the lack of PSI in *Viridis-zb63* the plants were extremely stressed, and hence the maximum fluorescence measured were considerably lower than for healthy control plants. However, pre-processing the transients as shown here allows for a comparison of the shape of the transients despite this difference. It was evident that the I-step was completely absent in the OJIP transients from the *Viridis-zb63* mutant.

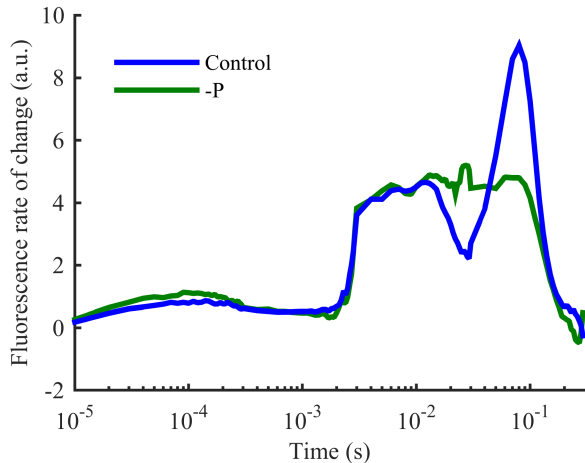


Figure S3: Differentiated, scaled and smoothed OJIP transients from barley. The I-step from a healthy control plant is seen as the clear depression at 0.03 s and subsequent large increase compared to the constant rate of change observed for the OJIP transient from the P deficient plant. All transients were similarly pre-processed prior to multivariate analysis.

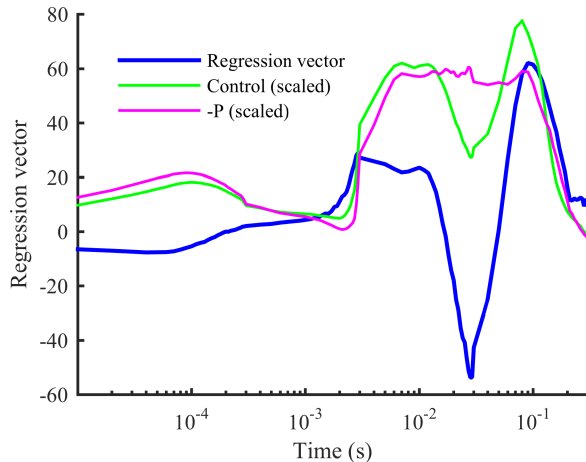


Figure S4: Regression vector for PLS model predicting the P concentration. For comparison, the pre-processed OJIP transients for a control and P deficient barley plant is included (scaled to match the amplitude of the regression vector). It is seen that high PLS predictions correspond to a noted I-step depression (at 0.03 s where the regression vector is negative) and subsequent increase.

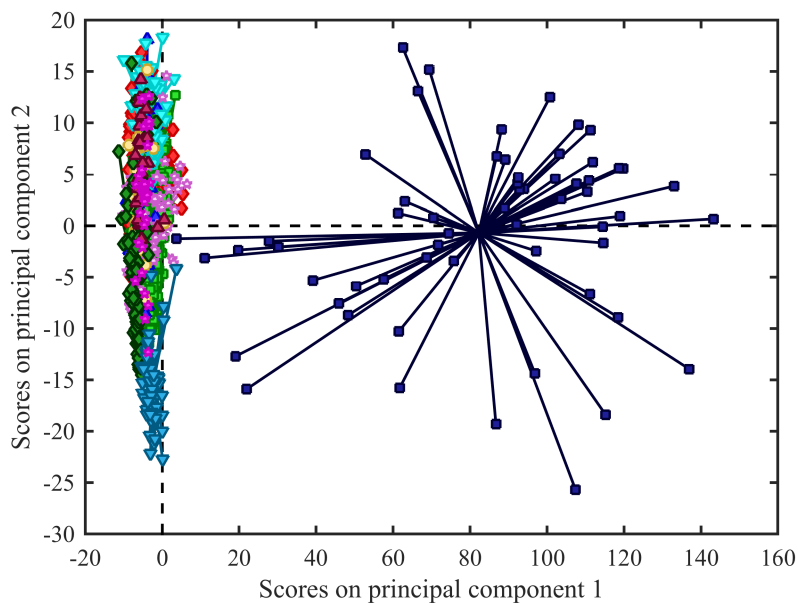
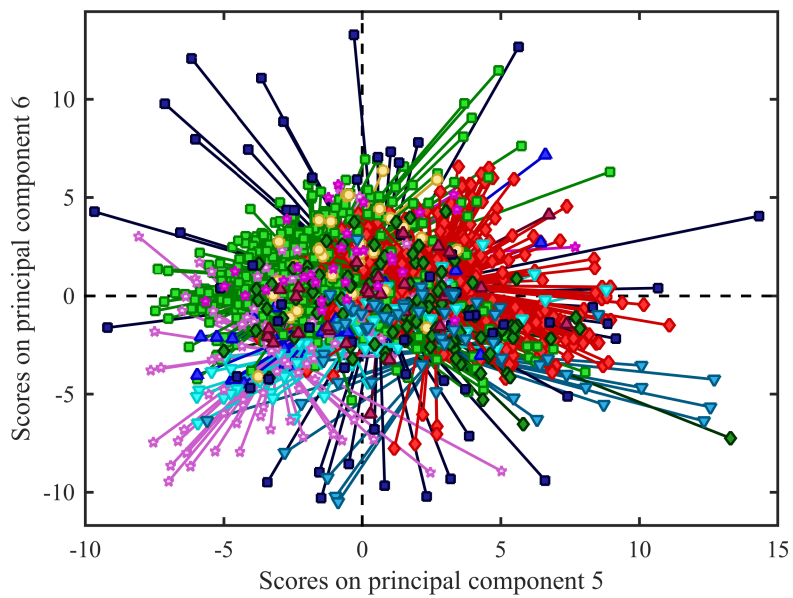
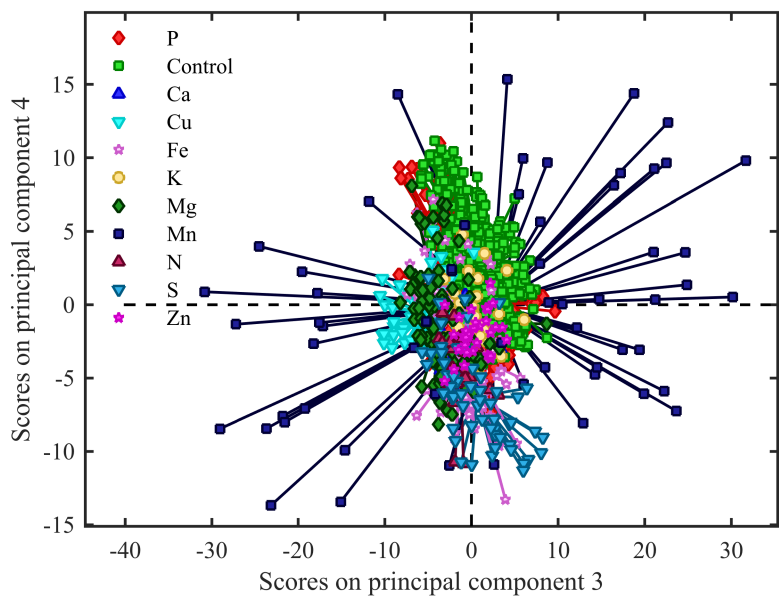


Figure S5: Principal components 1-2 (top), 3-4 (middle) and 5-6 (bottom). PC 1 explains 75.4% of the variance, PC 2: 10.0%, PC3: 4.6%, PC4: 3.2 %, PC5: 2.6 % and PC6: 1.8% of the variance. Mn deficiency is seen to dominate the overall OJIP variability seen in the dataset with clear clustering in PC1 scores, but other PC subspaces show clustering of varying strength of P, S, Cu, Fe and Mg.



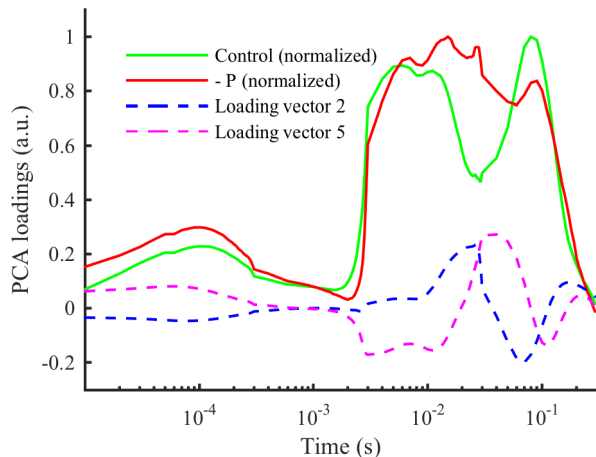


Figure S6: PCA loading vectors 2 and 5 plotted together with pre-processed OJIP transients from a control and P deficient barley plant (scaled to a maximum amplitude of 1 for comparison with the loadings vectors). It is evident from the loading vectors that principal components (PC's) 2 and 5 primarily depend on variations in the shape of the I-step. This corroborates the connection between a change in shape of the OJIP transient around the I-step, and plants suffering from P deficiency as the P deficient plants were seen to cluster distinctly from other deficiencies when plotting the scores of PC's 2 and 5. PC 2 explains 10.0 % of the variation, PC 5 explains 2.6% of the variation.

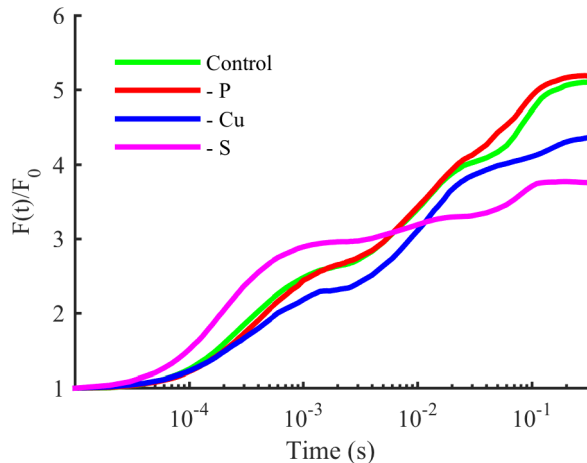


Figure S7: Non-processed OJIP transients (normalized by F_0) from a control (green) and a P, Cu and S deficient plant (including both barley and tomato plants). It is evident why both P, Cu and S deficient plants are seen to cluster in a score plot of principal components 2 and 5 as all three appear to affect the shape of the OJIP transient at the I-step, but in different ways. Cu deficiency appear to cause a lower overall increase from the I to P step, whereas S deficient plants appear to have a lower increase between J and I, yet a more pronounced I-step compared to even the control plant. While this strongly suggests that Cu and S deficiency can also be predicted based on OJIP transients, it does not appear to interfere with the effect of P on the shape of the OJIP transient.

Table S1: Elemental concentrations in the YFDL as obtained by ICP-OES. ‘A’ designates normal temperature and light, ‘B’ designates low temperature and high light. P1-P3 indicates decreasing levels of supplied P. W3-W6 indicates weeks where pots were resupplied with P, -P did not receive additional P. In experiment 2, plants were resupplied with P at 28 DAT. The results are average mass concentration in dry matter \pm standard deviation (n=4 or 5).

		P (%)	Ca (%)	K (%)	Mg (%)	S (%)	Fe ($\mu\text{g/g}$)	Mn ($\mu\text{g/g}$)	Zn ($\mu\text{g/g}$)		
Experiment 1 (n=4), hydroponics	21 DAT	Control	0.72 \pm 0.01	0.95 \pm 0.12	7.05 \pm 0.28	0.40 \pm 0.03	0.57 \pm 0.03	90 \pm 5	70 \pm 15	60 \pm 5	
		A	P1	0.37 \pm 0.03	1.00 \pm 0.04	7.24 \pm 0.45	0.41 \pm 0.02	0.66 \pm 0.01	110 \pm 15	100 \pm 5	80 \pm 5
		P2	0.20 \pm 0.01	0.84 \pm 0.04	7.85 \pm 0.33	0.34 \pm 0.02	0.54 \pm 0.02	100 \pm 10	100 \pm 15	85 \pm 10	
		P3	0.12 \pm 0.01	0.49 \pm 0.02	8.24 \pm 0.12	0.22 \pm 0.01	0.42 \pm 0.02	80 \pm 5	100 \pm 5	90 \pm 5	
		B	Control	0.41 \pm 0.04	0.63 \pm 0.09	4.24 \pm 0.33	0.23 \pm 0.02	0.44 \pm 0.05	60 \pm 5	40 \pm 10	30 \pm 5
		P1	0.24 \pm 0.05	0.43 \pm 0.10	5.12 \pm 0.73	0.17 \pm 0.03	0.45 \pm 0.08	70 \pm 10	35 \pm 10	50 \pm 10	
	28 DAT	P2	0.13 \pm 0.01	0.50 \pm 0.08	5.83 \pm 0.45	0.19 \pm 0.03	0.39 \pm 0.05	80 \pm 5	50 \pm 10	60 \pm 5	
		P3	0.09 \pm 0.01	0.53 \pm 0.04	7.71 \pm 0.21	0.23 \pm 0.03	0.37 \pm 0.01	100 \pm 60	100 \pm 10	105 \pm 30	
		A	Control	0.58 \pm 0.06	0.78 \pm 0.18	5.53 \pm 0.66	0.35 \pm 0.05	0.61 \pm 0.05	85 \pm 5	45 \pm 10	45 \pm 10
		P1	0.16 \pm 0.01	0.75 \pm 0.05	6.36 \pm 0.36	0.35 \pm 0.02	0.52 \pm 0.03	85 \pm 5	75 \pm 10	50 \pm 10	
		P2	0.11 \pm 0.02	0.61 \pm 0.13	7.50 \pm 0.20	0.28 \pm 0.05	0.44 \pm 0.04	85 \pm 15	80 \pm 20	60 \pm 10	
		P3	0.06 \pm 0.01	0.63 \pm 0.05	8.81 \pm 0.38	0.30 \pm 0.01	0.38 \pm 0.02	80 \pm 5	130 \pm 20	90 \pm 5	
Experiment 2 (n=4), hydroponics	21 DAT	Control	0.41 \pm 0.04	0.65 \pm 0.21	4.67 \pm 0.25	0.20 \pm 0.05	0.43 \pm 0.10	70 \pm 10	30 \pm 10	30 \pm 5	
		A	P1	0.11 \pm 0.01	0.45 \pm 0.11	5.76 \pm 0.46	0.16 \pm 0.03	0.36 \pm 0.05	70 \pm 20	35 \pm 10	40 \pm 10
		P2	0.09 \pm 0.02	0.55 \pm 0.05	6.80 \pm 0.46	0.18 \pm 0.02	0.39 \pm 0.02	70 \pm 10	55 \pm 5	55 \pm 5	
		P3	0.06 \pm 0.01	0.52 \pm 0.03	7.96 \pm 0.37	0.24 \pm 0.01	0.38 \pm 0.03	80 \pm 30	100 \pm 5	95 \pm 10	
	23 DAT	Control	0.62 \pm 0.04	1.04 \pm 0.40	8.36 \pm 0.45	0.46 \pm 0.16	0.40 \pm 0.03	75 \pm 5	160 \pm 100	105 \pm 55	
		P1	0.54 \pm 0.08	1.17 \pm 0.33	8.09 \pm 0.57	0.51 \pm 0.12	0.43 \pm 0.02	80 \pm 10	215 \pm 85	150 \pm 50	
		P2	0.21 \pm 0.04	1.30 \pm 0.05	7.54 \pm 0.40	0.58 \pm 0.01	0.44 \pm 0.01	75 \pm 10	250 \pm 25	150 \pm 10	
		P3	0.12 \pm 0.07	0.95 \pm 0.24	6.98 \pm 1.62	0.44 \pm 0.11	0.39 \pm 0.07	60 \pm 15	190 \pm 60	125 \pm 40	
	28 DAT	Control	0.70 \pm 0.11	0.54 \pm 0.23	8.17 \pm 0.32	0.28 \pm 0.07	0.45 \pm 0.02	70 \pm 5	65 \pm 25	75 \pm 10	
		P1	0.44 \pm 0.06	0.35 \pm 0.02	7.77 \pm 0.18	0.21 \pm 0.01	0.43 \pm 0.02	60 \pm 5	50 \pm 5	65 \pm 5	
		P2	0.24 \pm 0.05	0.47 \pm 0.29	7.20 \pm 0.91	0.23 \pm 0.10	0.41 \pm 0.02	70 \pm 10	80 \pm 45	80 \pm 10	
		P3	0.12 \pm 0.04	0.70 \pm 0.26	7.46 \pm 0.24	0.32 \pm 0.09	0.38 \pm 0.02	70 \pm 10	120 \pm 30	100 \pm 10	
30 DAT	Control	0.65 \pm 0.04	0.42 \pm 0.08	6.05 \pm 0.63	0.26 \pm 0.02	0.53 \pm 0.04	70 \pm 5	30 \pm 5	65 \pm 25		
	P1	0.17 \pm 0.04	0.62 \pm 0.15	7.11 \pm 0.76	0.29 \pm 0.05	0.47 \pm 0.06	70 \pm 10	90 \pm 30	70 \pm 15		
	P2	0.11 \pm 0.01	0.43 \pm 0.16	6.40 \pm 0.20	0.21 \pm 0.04	0.37 \pm 0.04	70 \pm 10	75 \pm 30	65 \pm 15		
	P3	0.09 \pm 0.01	0.33 \pm 0.08	6.65 \pm 0.33	0.18 \pm 0.04	0.33 \pm 0.02	60 \pm 10	75 \pm 25	75 \pm 10		
Experiment 3 (n=5), soil	Week 3	Control	0.60 \pm 0.11	0.62 \pm 0.27	7.10 \pm 0.24	0.32 \pm 0.07	0.47 \pm 0.03	60 \pm 5	50 \pm 15	65 \pm 25	
		P1	0.89 \pm 0.13	0.64 \pm 0.22	7.64 \pm 0.52	0.29 \pm 0.06	0.47 \pm 0.04	60 \pm 5	85 \pm 35	70 \pm 20	
		P2	1.03 \pm 0.17	0.47 \pm 0.12	8.00 \pm 0.23	0.23 \pm 0.03	0.41 \pm 0.02	60 \pm 5	70 \pm 15	70 \pm 10	
		P3	1.09 \pm 0.20	0.33 \pm 0.07	7.73 \pm 0.27	0.19 \pm 0.03	0.39 \pm 0.03	50 \pm 10	70 \pm 15	80 \pm 15	
		Control	0.72 \pm 0.05	0.80 \pm 0.08	6.78 \pm 0.66	0.17 \pm 0.01	0.46 \pm 0.01	80 \pm 5	55 \pm 5	45 \pm 5	
		W3	0.47 \pm 0.07	0.85 \pm 0.15	7.27 \pm 0.93	0.16 \pm 0.02	0.47 \pm 0.05	90 \pm 10	75 \pm 15	60 \pm 10	
		W4	0.48 \pm 0.12	1.01 \pm 0.22	8.02 \pm 1.11	0.17 \pm 0.04	0.47 \pm 0.04	95 \pm 20	80 \pm 15	70 \pm 10	
	Week 4	W5	0.40 \pm 0.09	1.06 \pm 0.24	7.10 \pm 0.74	0.17 \pm 0.03	0.47 \pm 0.05	90 \pm 15	80 \pm 15	50 \pm 10	
		W6	0.60 \pm 0.10	0.92 \pm 0.29	7.81 \pm 1.46	0.19 \pm 0.05	0.53 \pm 0.06	105 \pm 25	80 \pm 15	65 \pm 15	
		-P	0.51 \pm 0.15	0.84 \pm 0.15	7.40 \pm 0.82	0.17 \pm 0.03	0.48 \pm 0.06	95 \pm 20	70 \pm 10	60 \pm 20	
		Control	0.71 \pm 0.09	1.04 \pm 0.30	6.86 \pm 1.06	0.22 \pm 0.04	0.54 \pm 0.06	100 \pm 10	90 \pm 20	55 \pm 5	
		W3	0.47 \pm 0.13	1.12 \pm 0.34	7.03 \pm 0.67	0.19 \pm 0.01	0.48 \pm 0.04	95 \pm 15	120 \pm 30	55 \pm 10	
W4		0.39 \pm 0.05	0.96 \pm 0.13	6.69 \pm 0.59	0.17 \pm 0.02	0.46 \pm 0.03	100 \pm 10	105 \pm 10	60 \pm 5		
W5		0.37 \pm 0.09	0.98 \pm 0.25	6.84 \pm 0.65	0.16 \pm 0.03	0.45 \pm 0.04	100 \pm 15	110 \pm 30	55 \pm 10		
Week 5	W6	0.35 \pm 0.10	1.26 \pm 0.16	7.93 \pm 0.66	0.20 \pm 0.03	0.47 \pm 0.03	100 \pm 15	135 \pm 10	60 \pm 10		
	-P	0.41 \pm 0.08	0.81 \pm 0.11	6.68 \pm 0.62	0.18 \pm 0.02	0.50 \pm 0.03	110 \pm 15	100 \pm 15	65 \pm 10		
	Control	0.75 \pm 0.16	1.75 \pm 0.77	4.60 \pm 1.18	0.29 \pm 0.09	0.58 \pm 0.11	110 \pm 25	160 \pm 70	55 \pm 15		
	W3	0.83 \pm 0.07	1.50 \pm 0.80	5.77 \pm 0.95	0.26 \pm 0.04	0.56 \pm 0.05	110 \pm 10	165 \pm 60	60 \pm 5		
	W4	0.63 \pm 0.26	1.20 \pm 0.36	5.43 \pm 0.85	0.20 \pm 0.03	0.48 \pm 0.09	90 \pm 20	150 \pm 30	55 \pm 20		
	W5	0.43 \pm 0.05	1.02 \pm 0.36	6.21 \pm 0.81	0.19 \pm 0.03	0.53 \pm 0.07	90 \pm 15	160 \pm 35	55 \pm 10		
	W6	0.56 \pm 0.12	0.71 \pm 0.14	6.61 \pm 1.24	0.17 \pm 0.03	0.51 \pm 0.09	105 \pm 15	125 \pm 15	65 \pm 15		
Week 6	-P	0.44 \pm 0.08	1.00 \pm 0.46	6.11 \pm 1.27	0.19 \pm 0.05	0.47 \pm 0.06	90 \pm 30	130 \pm 40	60 \pm 15		
	Control	0.50 \pm 0.04	0.77 \pm 0.19	2.68 \pm 0.39	0.15 \pm 0.02	0.37 \pm 0.04	70 \pm 10	70 \pm 20	30 \pm 5		
	W3	0.53 \pm 0.22	1.00 \pm 0.28	3.62 \pm 1.48	0.17 \pm 0.03	0.41 \pm 0.08	75 \pm 15	110 \pm 35	35 \pm 10		
	W4	0.47 \pm 0.07	0.84 \pm 0.22	3.50 \pm 0.33	0.16 \pm 0.01	0.40 \pm 0.03	70 \pm 5	100 \pm 15	35 \pm 5		
	W5	0.63 \pm 0.07	1.24 \pm 0.29	3.36 \pm 0.41	0.17 \pm 0.02	0.39 \pm 0.05	70 \pm 10	170 \pm 50	30 \pm 5		
	W6	0.18 \pm 0.08	1.19 \pm 0.43	3.58 \pm 0.58	0.15 \pm 0.02	0.37 \pm 0.04	70 \pm 5	155 \pm 40	30 \pm 5		
	-P	0.16 \pm 0.05	1.14 \pm 0.40	3.82 \pm 0.52	0.17 \pm 0.02	0.39 \pm 0.05	75 \pm 10	155 \pm 50	30 \pm 5		

Table S2: Harvest data for experiment 1 which was used as calibration dataset. Biomass data are g fresh weight (FW). ‘A’ designates normal light and temperature conditions; ‘B’ designates high light and low temperature conditions. P1-P3 indicates treatments with decreasing levels of supplied P. The results are average \pm standard deviation (n=12).

		Shoot (g FW)	Root (g FW)	Root/Shoot	Tillers	Chlorophyll (mg/g FW)	Carotenoids (mg/g FW)	
21 DAT	A	Control	4.2 \pm 0.8	2.2 \pm 0.6	0.5	4	2.5 \pm 0.1	0.4 \pm 0.02
		P1	3.4 \pm 0.4	3.0 \pm 0.7	0.9	3	2.6 \pm 0.1	0.3 \pm 0.02
		P2	3.0 \pm 0.6	2.7 \pm 0.5	0.9	3	2.4 \pm 0.2	0.3 \pm 0.03
		P3	1.5 \pm 0.3	2.4 \pm 0.4	1.5	2	2.1 \pm 0.2	0.3 \pm 0.02
	B	Control	4.1 \pm 0.5	3.9 \pm 0.8	0.9	5	2.0 \pm 0.1	0.3 \pm 0.02
		P1	3.6 \pm 0.6	3.5 \pm 0.9	1.0	4	2.0 \pm 0.3	0.3 \pm 0.04
		P2	3.0 \pm 0.4	3.6 \pm 0.8	1.2	3	2.3 \pm 0.2	0.4 \pm 0.02
		P3	2.1 \pm 0.4	3.0 \pm 0.6	1.4	3	1.9 \pm 0.2	0.4 \pm 0.02
28 DAT	A	Control	9.4 \pm 1.4	4.2 \pm 1.3	0.5	6	2.6 \pm 0.2	0.4 \pm 0.04
		P1	6.0 \pm 0.9	3.7 \pm 0.6	0.6	5	2.7 \pm 0.2	0.4 \pm 0.02
		P2	4.6 \pm 1.0	3.4 \pm 0.8	0.7	4	2.4 \pm 0.2	0.4 \pm 0.03
		P3	2.2 \pm 0.5	3.0 \pm 0.4	1.4	2	2.0 \pm 0.2	0.3 \pm 0.02
	B	Control	9.8 \pm 2.1	6.8 \pm 3.4	0.7	7	2.3 \pm 0.2	0.4 \pm 0.03
		P1	5.9 \pm 1.0	5.0 \pm 2.1	0.8	6	2.0 \pm 0.2	0.4 \pm 0.04
		P2	4.4 \pm 0.9	5.4 \pm 1.2	1.2	5	1.9 \pm 0.1	0.4 \pm 0.04
		P3	2.3 \pm 0.4	3.2 \pm 0.6	1.4	3	1.7 \pm 0.1	0.3 \pm 0.02

Table S3: Results of field trials performed at 16 different locations in Denmark over two consecutive years. Average P concentrations (% in dry matter) at day 30 of the YFDL are shown for plots where no P fertilizer was added (-P), and plots where P fertilizer was added corresponding to 30 kg P ha⁻¹ placed below the seeds (+P). Relative grain yield shows the yield of the -P treatment relative to the grain yield from plots that received P fertilizer. A significant (P<0.05) decrease in relative grain yield is observed for the locations highlighted in bold font. For these locations, the P concentration in the YFDL for the -P treatment is ≤0.20%. At location DK 1, no yields loss is observed despite a P concentration <0.20%, this indicates that P is not the limiting nutrient. No consistent reduction in relative yield is observed for leaf P concentrations above 0.23% in the YFDL. (n=4 except for those marked with †, here n=3).

Location	P in YFDL (-P) day 30 (%)	P in YFDL (+P) day 30 (%)	Relative grain yield
DK 1	0.18±0.02	0.24±0.04 [†]	1.00±0.06
DK 2	0.20±0.01	0.24±0.01	0.92±0.04
DK 3	0.32±0.02	0.48±0.02	1.00±0.08
DK 4	0.28±0.10 [†]	0.39±0.05	1.02±0.05
DK 5	0.16±0.03	0.31±0.03	0.86±0.11
DK 6	0.15±0.07	0.26±0.02	0.81±0.10
DK 7	0.33±0.02	0.36±0.02	0.99±0.07
DK 8	0.25±0.01	0.27±0.02	0.95±0.08
DK 9	0.26±0.02	0.34±0.04	0.96±0.07
DK 10	0.30±0.03	0.35±0.02	0.95±0.08
DK 11	0.43±0.06	0.43±0.05	1.01±0.05
DK 12	0.23±0.02	0.28±0.01	0.98±0.02
DK 13	0.26±0.04	0.24±0.01	0.98±0.05
DK 14	0.42±0.04	0.49±0.03	0.93±0.07
DK 15	0.43±0.02	0.45±0.03	1.01±0.04
DK 16	0.42±0.01	0.42±0.12	0.96±0.06